Orthogonal Codes for CDMA-based Asynchronous Medical Wireless Body Area Networks (WBANs)

by

Ali Tawfiq

A thesis submitted in conformity with the requirements
for the degree of Masters of Applied Science (M.A.Sc)
The Edward S. Rogers Sr. Department of Electrical and Computer Engineering
University of Toronto

Your file Votre référence
ISBN: 978-0-494-93049-6

Our file Notre référence
ISBN: 978-0-494-93049-6

Abstract

Orthogonal Codes for CDMA-based Asynchronous Medical Wireless Body Area Networks (WBANs)

Ali Tawfiq

Masters of Applied Science (M.A.Sc)

The Edward S. Rogers Sr. Department of Electrical and Computer Engineering

University of Toronto

2012

The presented work considers a CDMA-based Wireless Body Area Network (WBAN) where multiple biosensors communicate simultaneously to a central node in an asynchronous fashion. The asynchronous nature of the WBAN introduces Multiple Access Interference (MAI). To combat this problem, presented is a methodology that uses a set of cyclically orthogonal spreading codes extracted from the Walsh-Hadamard matrix. When using the Cyclic Orthogonal Walsh-Hadamard Codes (COWHC) as spreading codes in the CDMA-based WBAN, the cyclic orthogonality property helps mitigate MAI amongst the on-body sensors. Presented is an ideal communication system that is most effective at mitigating MAI in proactive WBANs. The work illustrates the system optimality and effectiveness at mitigating MAI by studying the sensitivity to packet-loss through simulating the link Bit Error Rate (BER) performance. It is shown that the proposed design with COWHC, a Rayleigh flat-fading channel, BPSK modulation and a conventional receiver produce optimum MAI mitigation.

Dedication

The contents, long hours, knowledge, and commitment shown herein were only possible because of my family. I dedicate this to my father and role model Raied, mother and teacher Fetooh, my brother and mentor Mohammad, my sisters and sweethearts Marwa and Nora, and my dearest grandmother Nooria.

Thank You from the bottom of my heart

Acknowledgements

I would like to express my sincere appreciation to my supervisor Professor Konstantinos N. Plataniotis for all the support, knowledge, guidance and mentorship he has provided for the duration of my research life. Without his kind support and enthusiasm during my M.A.Sc and B.A.Sc studies, my research career would not have been the same. For that I am forever grateful.

I would also like to express my sincere thanks to Dr. Jamshid Abouei for all the knowledge and expertise that he provided to me during my M.A.Sc studies. This project would not have gone this far without the endless discussions and comments he continuously provided for the duration of this research.

Last but not least, I would like to thank all my colleagues at the department, and especially those in the Multimedia Laboratory. Special thanks to my dear colleagues Mahdi Hosseini and Amir Aghaei, without your continued technical, theoretical, and moral support all of this would not have been possible.

Contents

List of Acronyms

ADC	Analog-to-Digital Converter
ASK	Amplitude Shift Keying
AWGN	Additive White Gaussian Noise
BAN	Body Area Network
BER	Bit-Error-Rate
BPSK	Binary Phase Shift Keying
CCU	Central Control Unit
CDMA	Code Division Multiple Access
COWHC	Cyclic Orthogonal Walsh-Hadamard Codes
DBPSK	Differential Binary Phase Shift Keying
DQPSK	Differential Quadrature Phase Shift Keying
DSSS	Direct Sequence Spread Spectrum
ECG	Electrocardiogram
EEG	Electroencephalogram
FCC	Federal Communication Commission
FDMA	Frequency Division Multiple Access
FFD	Full Function Device
FSK	Frequency Shift Keying
FWHT	Fast Walsh-Hadamard Transform
GMSK	Gaussian Minimum Shift Keying
HBC	Human Body Communications
IDH	Intradialytic Hypotension
ISI	Inter-Symbol-Interference
LAN	Local Area Network

LOS	Line-of-Sight
LR-WPAN	Low Rate- Wireless Personal Area Network
MAC	Medium Access Control
MAI	Multiple Access Interference
MICS	Medical Implants Communication Services
MIMO	Multiple Input Multiple Output
MMSE	Minimum Mean Square Error
MUD	Multiple User Detection
NB	Narrowband
PAN	Personal Area Network
PDF	Probability Density Function
PHY	Physical Layer
PSK	Phase Shift Keying
OQPSK	Offset Quadrature Phase Shift Keying
QoS	Quality of Service
QPSK	Quadrature Phase Shifty Keying
RFD	Reduced Function Device
RMS	Root Mean Square
SNR	Signal-to-Noise Ratio
SUD	Single User Detection
TDMA	Time Division Multiple Access
UWB	Ultra Wide Band
WBAN	Wireless Body Area Networks
WLAN	Wireless Local Area Network
WMTS	Wireless MedicalTelemetry Services
WSN	Wireless Sensor Network
WWSS	Wearable Wireless Sensor System

List of Tables

List of Figures

List of Notations

Throughout this document, normal letters are used to denote scalars. Boldface capital and lower case letters denote matrices and vectors, respectively. The transposition and the conjugated transposition of a complex matrix $\mathbf{A}$ are denoted by $\mathbf{A}^T$ and $\mathbf{A}^\dagger$, respectively. The $n \times n$ identity matrix is denoted by $\mathbf{I}_n$. Operators with "$\circledcirc$" correspond to the decoded signal at the CCU of their counterpart at the transmitter. $\mathbb{E}[\ .\ ]$ represents the expectation operator. Also, E and T are used for energy and time parameters, respectively. Also, $\mathcal{A}_i$ is the i^{th} row of size $n \times n$ matrix $\mathcal{A}$, i.e. $\{\mathcal{A}_i\} \equiv \{a_{ij}\}_{j=1}^{n}$. For convenience, a list of key mathematical symbols used in this document are provided in Table 1.

Table 1: List of Notations

B: Channel bandwidth	f_c: Center frequency
d: Transmission distance	E_s: Symbol energy
K: Total number of biosensors	E_b: Bit energy
M: Constellation size	h_i: Fading channel coefficient
X_i: Raw digital message	$\mathcal{L}_d$: Channel gain factor with distance d
L_i: Size of bit message	T_b: Message bit duration
m_l: Message bit value	T_c: Chip duration
$\mathcal{X}_i$: Received signal at CCU	T_{sl}: Sleep mode duration
$\mathcal{S}_i$: i^{th} biosensor	T_{ac}: Active mode duration
s_i: Modulate signal for i^{th} sensor	T_{tr}: Transient mode duration
w_i: Spreading code for i^{th} sensor	T_s: Symbol duration
η: AWGN	λ: Wavelength
N: Processing gain	$\mathcal{G}$: Antenna Gain
$\mathbf{H}_{2^k}$: Hadamard matrix	ξ: Path-loss exponent
$\mathbf{W}\left(2^k, k\right)$: Walsh-Hadamard Codes	$\Omega = \mathbb{E}\left[\lvert h_i \rvert^2\right]$
$\mathbb{E}[\ .\ ]$: Expectation operator	R_{xy}: Cross-correlation between x and y
θ: Code phase-shift	

Chapter 1

Introduction

This thesis studies the problem of packet collision and multiple access interference in CDMA-based wireless body-centric networks. This chapter begins by introducing the advancement in both the industrial field and wireless communications that stresses the importance of wireless networking in the medical field. Then, the motivations and challenges in solving the problem is discussed. Finally, the proposed solution for multiple access and packet collision mitigation is reviewed and a road map to the rest of thesis is given.

1.1 Introduction to WBANs

In recent years advancements in the development of low-power electronics, sensing devices, wired and wireless technologies has been on the rise as demand for improved services in sectors such as healthcare has surged. Wireless communication for example has seen a tremendous overhaul in the past decade as it became a preference over wired communication in many applications. Anything from satellite communication, television, telephony, Internet, personal gadgets and even electricity are all applications of wireless communication. The advances in technology and that of wireless communication has led to the development of solutions that caters to the healthcare industry while effectively

and reliably complimenting the work done by professional healthcare personnels. This includes but is not limited to the: development of accurate sensing devices, designing wireless monitoring devices to allow for remote monitoring, and advancing medical networking capabilities within the hospital environment. Wireless communication is used in healthcare institutions and are utilized in pagers, wireless monitoring devices, and wireless sensors and are in continuous operation by staff and patients alike. The development of low-power, small medical sensing devices that are capable of monitoring the physiological nature of the human body coupled with the advancement in wireless communication and software engineering has led to the integration of such technologies in ubiquitous healthcare systems. The introduction of cheap, reliable and wearable sensing devices allowed for the development of small wireless networks capable of continuously monitoring patients in hospital beds, in the vicinity of the hospital, or even at the comfort of their home. These sensors create closed wireless networks named Wireless Body Area Networks that continuously observe the physiological state of patients.

Wireless Body Area Networks (WBANs) support a broad range of medical/non-medical applications in healthcare, medicine, and sports. Of interest is the use of WBANs for the continuous monitoring of physiological signals for both diagnosis and prevention [6, 7]. Those include on-body measurements such as the Electrocardiogram (ECG), Electroencephalogram (EEG), temperature and blood pressure, and/or accurate diagnosis of vital signs of the patients' in-body by implantable sensors [4, 8]. The operation and design of the sensor network and its respective components are governed by medical and industrial regulations. These regulations ensure maximum safety to the patient, reliability in communication, and accurate measurements of the physiological signals. Anything from power sources, sensing devices, cables, and wireless transceivers are bound by such regulations. Given the fact that the patients' well being might be dependent on the accurate realization of such networks, a high level of design and implementation accuracy is maintained throughout the system. Several factors must be taken into consideration

in the design and implementation of WBANs, including the modelling of the body area channel and choosing an appropriate protocol design matched with the network topology. On the other hand, since WBANs are known as short range communications, circuits energy consumption are comparable to the RF transmission energy, which requires the devices to be simple and have low-power consumption characteristics.

There is continuous high demand for wireless monitoring solutions and a variety of wireless protocols are continuously proposed and implemented to enhance the reliability of such networks, as well as support a wider range of medical devices [9]. Due to medical regulations, the protocols for WBANs must comply with the maximum transmit power, frequency of operation and the minimum interference posed on other medical devices. On the other hand, the protocols in such WBANs where multiple biosensors communicate to a central node must support high rate of reliability, immunity to noise and multiple access capabilities in a realistic channel model between the human body and the central node. Hence, WBAN devices must pose designs with low-power consumption characteristics while being highly robust to noise and interference to provide the desired long-term application.

1.2 Motivations and Challenges in WBAN design

When designing and implementing solutions such as WBANs that compliment the work of healthcare personnels, the design must achieve a high degree of sensing and diagnosis accuracy, while being both power and energy efficient. In order to achieve the operational standard set out by medical regulations and industry standards (further discussed in Chapter 2), the design of WBANs posses a number of technical challenges:

1. **Data and time asynchronicity:** In body-centric networks, each biosensor transmit its own information in a predetermined active mode duration which may be different from neighbouring sensors. This ensures that the sensors are asynchronous

in time. On the other hand, the data collection and transmission rates of the various sensors may be different from each other, as each could be sensing a different physiological signal. This introduces data rate asynchronicity to the network. This kind of time and data rate asynchronicity posses a design challenge particularly when several biosensors access a common transmission channel simultaneously. This leads to the collision of some packets at the central node and the loss of vital data at the receiver. The collided packets must then be retransmitted, which is considered a major source of energy waste in the network since *i*) a feedback channel must be established from the central node to the biosensor, and *ii*) power and energy is further consumed to reprocess and transmit the lost packets.

2. **Efficient spectrum utilization:** Wireless technologies utilize a large operating spectrum (∼30KHz to 300GHz) as allocated by spectrum regulators such as Industry Canada (in Canada) and the Federal Communications Commission (FCC - in the USA) [10, 11]. Crowding a given allocated spectrum range can affect the overall quality of transmission by having many users accessing the same spectrum. An increase in demand for wireless spectrum can only be matched in one of two ways: (i) releasing higher frequency ranges, (ii) enhancing existing techniques to better utilize the wireless spectrum. Releasing higher frequency ranges is both economically expensive and requires higher and more sophisticated computational complexity. On the other hand we can modify and enhance existing wireless techniques to better utilize the allocated spectrum for any given application. And such is the case for WBANs, given the devices and network operating environment and the frequency range provided by spectrum regulators, it is crucial to utilize wireless protocols that efficiently use the given spectrum. Of interest is the use of multiple-access protocols such as Time Division Multiple Access (TDMA), Frequency Division Multiple Access (FDMA), and Direct Sequence Code Division Multiple Access (DS-CDMA) with orthogonal spreading codes.

3. **Spreading code orthogonality:** One challenge faced in CDMA-based WBANs is the utilization of proper spreading codes with minimum mutual cross-correlation to mitigate Multiple Access Interference (MAI). However, the problem in using spreading codes is the loss of orthogonality due to the time and data asynchronicity and/or multi-path signal propagation. This loss of orthogonality will further contribute to the problem of multiple access interference and increase the decoding error rate probability. Of interest is studying the optimality of spreading codes with orthogonality properties resilient to the asynchronicity of the WBAN.

1.3 Contributions

This thesis aims to propose a communication system design for WBANs that tackles the challenges presented in Section 1.2. Of interest is the development of a wireless protocol that: *i*) has collision-free properties, *ii*) multipath resilient properties, *iii*) supports various data rates, and *iv*) uses available frequency and time resources efficiently [12]. The deliverables of this thesis is divided into the following two major contributions:

1. **Cyclically orthogonal spreading codes:** Given the effect of asynchronicity on the orthogonality of spreading codes in CDMA-based networks, the work presented in this thesis proposes the use of a special set of orthogonal Walsh-Hadamard spreading codes that are resilient to the asynchronous nature of WBANs. The Cyclic Orthogonal Walsh-Hadamard Codes (COWHC) are a subset of the conventional Walsh-Hadamard codes that maintain their orthogonality even when the sensor nodes are asynchronous in time, and have zero mutual cross-correlation for every time delay value. When used in the proposed CDMA-based WBAN, COWHC will mitigate the effect of MAI and effectively lower the detection Bit-Error-Rate (BER). This will ensure that the transmitted vital data is accurately decoded at the central node of the body network while power resources are reserved (no packet

retransmission is required). The optimality of COWHC is compared to conventional semi-orthognal spreading codes such as Gold codes [13] and chaotic codes [14].

2. **Asynchronous CDMA-based WBAN:** The idea is to design a communication system that can operate around the time and data asynchronicity of WBANs and can efficiently utilize the limited spectrum allocated for WBAN applications. In the study shown in Chapter 2, it is evident that utilizing a CDMA-based multiple access protocol where sensors are assigned unique orthogonal spreading codes to access a common channel simultaneously is the most promising. However, the majority of protocols used for cellular and classical wireless networks are not directly applicable to on-body wireless networks. Hence, the proposed network design studies the effect of multiple modulation schemes, receiver designs, and spreading parameters for a CDMA-based wireless on-body network that effectively mitigates MAI.

To the best of our knowledge, this is the first in-depth study in the physical layer of asynchronous CDMA-based WBANs which captures the effects of spreading codes, modulation techniques, and receiver structure on the link and network performance. The presented work differs from previous CDMA-based wireless sensor networking applications in two ways; *i*) the WBAN maintains the asynchronous operation and no power is consumed for transmission scheduling and no feedback channels are required, and *ii*) using COWHC for spreading does not require any specific code assignment algorithms to minimize MAI as all codes are mutually orthogonal to each other and produce zero cross-correlation.

1.4 Organization

The rest of the thesis is organized as follows:

Chapter 2 investigates the prior art in body centric wireless networks. First a detailed overview of the WBAN structure, existing applications and technical device specifications are presented. Then a comprehensive review of various wireless standards that cater to WBAN application is presented, and prior spread spectrum and CDMA-based WBAN are analyzed. Finally, a thorough definition of the problem to be solved is stated.

Chapter 3 presents a detailed overview of the proposed cyclic orthogonal Hadamard spreading codes. First, the theoretical background and orthogonality property of Walsh-Hadamard codes is reviewed. The cyclic orthogonal Hadamard codes are studied next. Then, the approach taken to validate the results presented in this document is provided as well as the simulation setup. Finally, simulation results in support of the proposed cyclic orthogonal codes is presented.

Chapter 4 provides a detailed account on the proposed CDMA-based WBAN. The details of the system model including data gathering, modulation and spreading mechanisms is presented. Then a study of the proposed channel model and receiver structures is provided. Finally, simulation results that examine the performance of the proposed system is presented.

Chapter 5 presents a discussion of the research results and findings provided in this document. A recommendation on the validity of the presented work is provided and possible future work to be conducted on this subject is also discussed.

Chapter 2

Review of Prior Art, Design, and Setup of WBANs

This chapter formulates the problem of MAI in WBANs by first providing an overview of WBANs from a system and application point of view. Then a study of the history of wireless medical standards used in WBANs is presented. Next, a detailed formulation of the application of spread spectrum in WBANs is provided. Finally the problem definition is reiterated and a summary of the chapter is presented.

2.1 Hierarchical Overview of Medical Networking

Body Area Networks (BANs) are networks that connect multiple biomedical sensing and monitoring devices in or around the vicinity of the human body. With the advancement of wireless technology, convenient Wireless Body Area Networks where the devices are wirelessly interconnected to each other and to the central node were developed. With the operation of WBANs around the human body in hospitals, healthcare institutions and homes, the wireless transmission is governed by wireless and medical regulations. BANs can support a variety of applications from sports to medical. Of interest is studying the implementation of WBANs from the wireless physical layer design in medical applications.

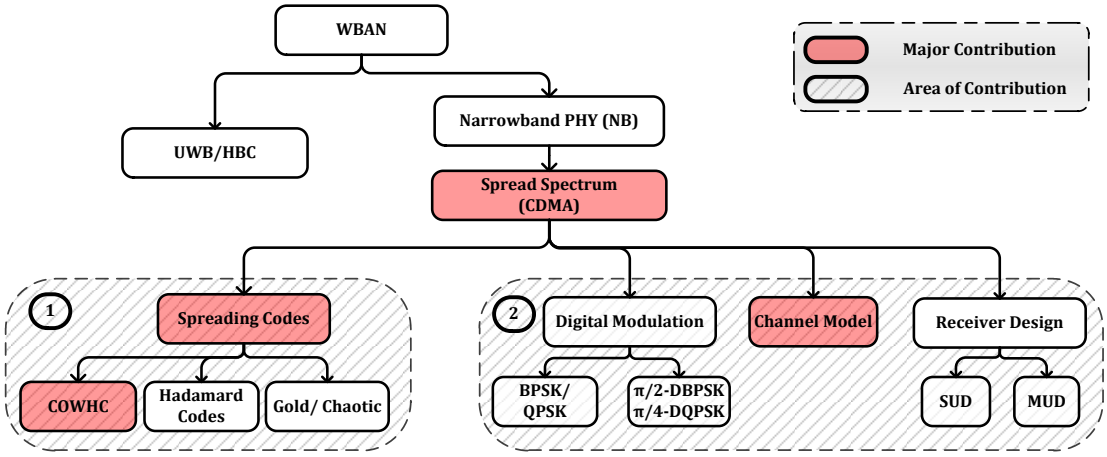

Figure 2.1: Overview flow diagram

As shown in the flow diagram in Figure 2.1, the Physical Layer (PHY) of WBANs can operate in two ways; Narrowband (NB), and Ultra-Wideband (UWB). Of interest is studying the operation of WBANs in the NB physical layer as it is primarily responsible for the *i*) activation and deactivation of radio transceivers, and *ii*) data transmission and reception, which will aid in the investigation of MAI at the bit level. To support multiple devices (users) within the WBAN, Direct Sequence Spread Spectrum (DSSS) techniques such as CDMA has been previously proposed in the literature [12, 15]. In CDMA-based WBANs each node is assigned a unique spreading code that spreads the signal over a larger bandwidth than that of the original message. This technique provides both security and a system design that can control the interference posed at each node by assigning orthogonal spreading codes to the network nodes. The areas of contributions presented in this thesis document are also shown in Figure 2.1, where the proposed COWHC spreading codes are compared to existing spreading codes used in CDMA-based WBANs and the proposed WBAN system is investigated from both the digital modulation and receiver design point-of-views.

2.2 The Design of Wireless Body Area Networks

This work considers a typical body centric wireless sensor network consisting of multiple biosensors that communicate wirelessly to a Central Control Unit (CCU). The network as shown in Figure 2.2 contains K on-body biosensors denoted by $\mathcal{S}_1$,$\mathcal{S}_2$,$\cdots$,$\mathcal{S}_K$ and the CCU. The total number of sensors in WBANs is typically very low, $2 \leq K \leq 10$, as to not compromise the comfort and regular activity of the user [16].The sensor nodes collect physiological data from on-body/ in-body sensors and transmit the data wirelessly to the CCU (the roles of two types of node is further explained in Section 2.2.2). The CCU on the other hand receives the data from multiple sensors in the network and decodes for the transmitted data. Given the nature of the design of WBANs, sensor nodes have power-constrained batteries contrary to the CCU which can have a power source. Hence there is a need to reduce the overall power consumption and computational complexity of the sensor nodes to prolong the lifetime of the network. For this purpose, WBANs utilize a duty-cycling mechanism such as the one illustrated in Section 2.2.1 which achieves a significant energy saving in both circuit and signal transmission [4].

2.2.1 Duty-Cycle Mechanism

In the CDMA-based WBANs, it is assumed that all biosensors utilize spreading codes with the same processing gain $N \triangleq \frac{T_b}{T_c}$ and the same modulation scheme, such that the average transmitted energy per symbol is the same for all nodes. It is also assumed that the biosensors are unaware of the other nodes' wake up processes. This makes the network be inherently tolerant to the failure of individual sensors. Under the above assumptions, the data transmission rates of all biosensors are the same. In [4] the authors present a proactive WBAN where each sensor periodically turns on its transmitter for T_{ac} every T_N seconds, the duty-cycle is defined as $\frac{T_{ac}}{T_N}$. During the active mode period of sensor $\mathcal{S}_i$, $T_{ac,i}$, the raw signal measured by the biosensor is first passed through the amplification and

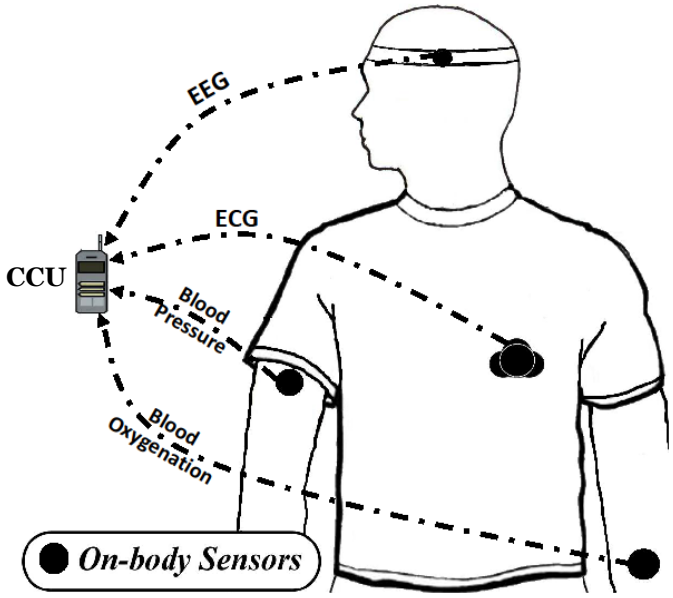

Figure 2.2: Wireless Body Area Network diagram

filtering processes to increase the signal strength and remove unwanted signals and noise. The filtered analog signal is then digitized by an Analog-to-Digital Converted (ADC), and an L_i -bit message sequence $X_i \triangleq \{m_\ell\}_{\ell=1}^{L_i}$ is generated, where $m_\ell \in \{-1, +1\}$ and L_i is assumed to be fixed for the node $\mathcal{S}_i$ and is not necessarily the same as L_j for the node $\mathcal{S}_j$, $j \neq i$. Without loss of generality and for ease of analysis, the authors assume that the bit duration of m_ℓ, denoted by T_b, is the same for all $\mathcal{S}_i$ nodes.

The $\mathcal{S}_i$ then returns to the sleep mode, and all the circuits of the transmitter are powered off for the sleep mode duration $T_{sl,i}$ for energy saving (see Figure 2.3). Denote T_{tr} as the transient mode duration consisting of the switching time from sleep mode to active mode (i.e., $T_{sl\to ac}$) plus the switching time from active mode to sleep mode (i.e., $T_{ac\to sl}$), where $T_{ac\to sl}$ is short enough compared to $T_{sl\to ac}$ to be negligible. Furthermore, the amount of power consumed for starting up the $\mathcal{S}_i$ is more than the power consumption during $T_{ac\to sl}$ [17].

The main advantage of the above duty-cycling process is the energy saving and the

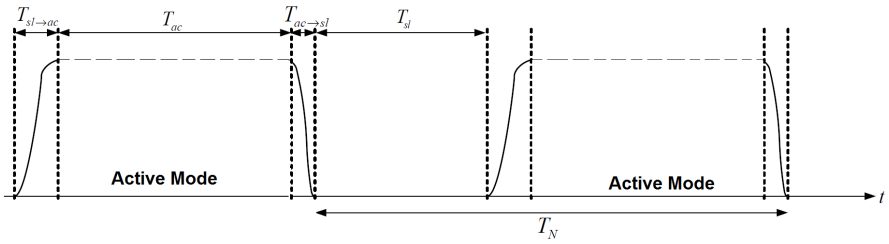

Figure 2.3: Practical duty-cyclic process in a proactive WBAN [4]

lower computational complexity over conventional CDMA schemes where all the nodes transmit the signal during the whole time slots. Since the biosensors in WBANs measure different physiological information, and noting that each sensor has its own active mode duration depending on the body signal characteristics, there exists an asynchronous duty-cycling mechanism from the whole network points of view (see Figure 3.6).

2.2.2 Network Topology

At the network level, there exists two types of nodes in WBANs:

- **Sensor node:**

  The objective of this unit is to gather and collect the intended physiological signal from the surface of the human body, or from an implant. It consists of the following components: power source (battery), sensor hardware, processor and either a transmitter or transceiver [18].

- **Central Control Unit:**

  This unit gathers all the transmitted information from multiple biosensors in the WBAN and processes the data for monitoring or diagnosis purposes [1]. This can either be a mobile device with a limited power supply, or a computing unit with a power source. Data can either be used locally, or further transmitted into a larger collection unit or a monitoring centre.

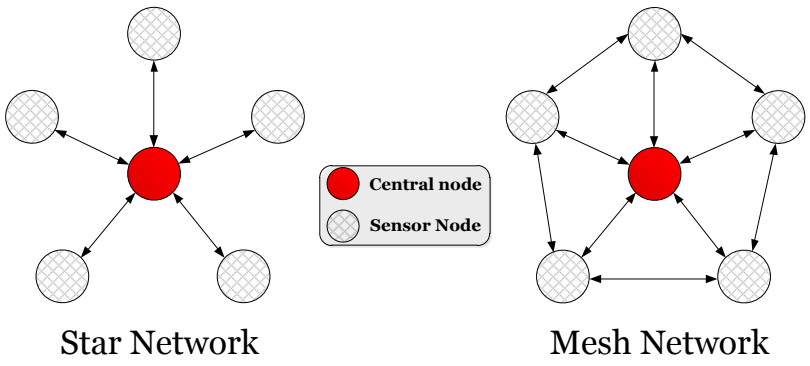

Figure 2.4: Network topologies for WBANs: (i) star network, and, (ii) mesh network

Typically, WBANs have multiple sensor nodes scattered around the vicinity of the patients body, while ideally there is one CCU for every WBAN. The sensor nodes and the CCU can be arranged into one of two network topologies as shown in Figure 2.4 [19]:

- **Star Network:**

  sensor nodes have unidirectional or bidirectional communication with the central node and no there exists no inter-node communication.

- **Mesh Network (peer-to-peer topology):**

  sensor nodes have bidirectional communication with the central node as well as each other.

In a star network configuration the sensor nodes wirelessly communicate to the CCU, and there exists no communication amongst the individual sensor nodes [20]. Given that sensor nodes operate on limited power and computation resources, some WBANs utilize unidirectional communication between the sensor nodes and the CCU to preserve battery [21]. While in a mesh Network configuration sensor nodes communicate to each other as well as the CCU, which would require a larger power source at the sensor nodes end.

In star networks, little signal processing is done at the nodes and typically raw signals produced from the sensors are amplified and converted to the digital format before pro-

ceeding to the transmitter block. This is done to lower the computational complexity at the sensor nodes and to ultimately reduce power consumption. Hence the transmitted raw signal is processed and analyzed at the CCU where there is less power constraints. Also due to the power-constrained nature of the sensor nodes, there exists no feedback channel from the CCU to the sensor nodes, and hence no synchronization or time-scheduling techniques are possible. This creates an asynchronous WBAN in nature where the sensor nodes will be transmitting their data over to the CCU at predefined intervals unknown to other nodes in the network.

2.2.3 Existing WBAN Applications

The usability of Wireless Body Area Networks has stretched into a number of applications in the medical field and have become a crucial part of both diagnosis and monitoring. In [22], the authors present a wireless monitoring system based on a WBAN that is targeted for the monitoring of dialysis patients. Intradialytic Hypotension (IDH) is a complication where a rapid decrease of blood pressure occurs as excess amounts of water are removed from the body during dialysis. IDH affects dialysis patients with diabetes and cardiovascular complications and may lead to nausea, vomiting and anxiety [23]. The authors propose the WBAN system for continuously monitoring patients during dialysis. The purpose of the WBAN is to automatically measure vital signs such as pulse, systolic and diastolic blood pressure and communicate an alert to a monitoring nurse if IDH occurs. While the system produced IDH detection success ratio of 94.841%, the authors raise an issue with data loss and packet collision in the WBAN and that future work must constitute techniques to lower overall packet collision in the WBAN and effectively increase the detection success rate.

In [24], the authors proposed a Wireless Sensor Network (WSN) aimed for real-time monitoring and detection of heart attacks. The intended Wearable Wireless Sensor System (WWSS) is designed such that ECG signals are continuously captured and transmit-

ted to the patient's mobile device and effectively alert doctors, relatives and near-by hospital staff of any cardiovascular complication. The authors propose the use of the system in remote areas where patients might not have immediate attention to life-threatening complications. The effective implementation of such WSN will decrease the risk of death to patients with heart complications while living in rural areas. It is also crucial that the wireless transmission in WWSS is reliable and does not produce false alerts due to packet loss or transmission errors.

Meanwhile research is being conducted to maintain low computational complexity in WBANs by introducing compression techniques as well as low-power sensing devices. In [25], the authors propose an ECG compression algorithm that permits lossless transmission of ECG over bandwidth limited wireless links such as SMS and MMS. Meanwhile introducing techniques for the detection of cardiovascular abnormalities from the compressed ECG data. This work allows for less bandwidth to be used for transmission all while creating an effective monitoring WBAN. Such technologies can be used in WBANs intended for real-time monitoring of cardiovascular signals such as the system presented in [26]. In [26], the authors present a WBAN that uses ZigBee based ECG devices [27] to develop continuous monitoring networks for Electrocardiogram activity using MATLAB.

It is evident that Wireless Body Area Networks are attracting a lot of attention for the enhancement of patient monitoring and diagnosis for a variety of medical needs. It is crucial that such WBANs are designed with the utmost attention to detail and that vital physiological information are reliably transmitted from the sensor nodes to collection units to avoid diagnosis and monitoring errors.

2.2.4 Typical WBAN Sensor Specifications

As shown in the previous section, WBANs can span a number of applications, each with a varying number of sensing devices. Sensors in WBANs have varying data rates depending on the nature of the physiological signal being monitored. In [1], the authors

Signal	**Data Rate**	**Bandwidth (Hz)**	**Parameter Range**
ECG (6 leads)	288 kbps	100-1000	0.5-4 mV
EEG (12 leads)	43.2 kbps	0-150	3 μV-300 μV
EMG	320 kbps	0-10000	10 μV-3 mV
SpO_2	16 bps	0-1	–
Temperature	120 bps	0-1	32-40 °C
Glucose monitor	1.6 kbps	0-50	–

Table 2.1: List of typical WBAN sensors and their technical specifications [1, 2]

present a number of standard data rates that govern a number of biosensors typically used in WBANs, and are shown in Table 2.1.

It is evident from Table 2.1 that biosensors utilized in WBANs operate with a variety of data rates and signal bandwidths. This variation in data rates and sensor technical specifications contribute to the asynchronicity of WBANs.

2.3 Wireless Standards for WBANs

As wireless telecommunication started to be implemented in hospitals and medical institutes, there were many calls for standardized protocols to be developed for medical applications. In 1999, a HDTV station performed a broadcasting test near the Baylor University Medical Center in Dallas, Texas, which occupied the same band as the hospital's medical telemetry, effectively making certain monitors inoperable [28]. This lead to increased calls for dedicating a band exclusively for wireless medical applications. Medical services used to operate on an unlicensed basis on TV channel bands, which made it prone to high levels of interference. Then a variety of medical specific wireless protocols have been developed and used for WBANs and other medical networking applications. The following is a list of such protocols, and technical details about these protocols can

be found in Appendix A:

1. Wireless Medical Telemetry Services (WMTS)
2. Wireless Local Area Network (WLAN)
3. Medical Implants Communication Services (MICS)
4. IEEE 802.15.4 - ZigBee
5. IEEE 802.15.6 - WBAN

The latest of the above is the IEEE 802.15.6, which is a standard specifically designed for low-power WBANs. This standard is of interest as it is likely to be the main standerdized protocol used in WBANs for the near future.

2.3.1 IEEE 802.15.6 - WBAN

IEEE 802 has established a Task Group called IEEE 802.15.6 to provide a standard specifically designed for Wireless Body Area Networks [29]. The standard is intended for communication optimized for low-power in-body/ on-body sensors in WBANs. It serves a number of medical and non-medical based WBANs. This yet to be published standard will meet low power operation, Quality-of-Service (QoS) and interference requirements set by medical regulators. It is planned that IEEE 802.15.6 will be an internationally recognized standard for WBANs as it defines a Medium Access Control (MAC) for several physical layer designs for WBANs. Of interest is the three PHY designs proposed in IEEE 802.15.6: Narrowband (NB), Ultra Wideband PHY (UWB), and, Human Body Communications (HBC) [30].

The Narrowband PHY is responsible for activation and deactivation as well as data transmission and reception. It supports a number of bands: 402-405 MHz, 420-450 MHz, 863-870 MHz, 902-928 MHz, 950-956 MHz, 2360-2400 MHz, and 2400-2483.5 MHz. In

	WMTS	WLAN	MICS	ZigBee	802.15.6
Frequency Bands	608-614 MHz 1395-1400 MHz 1427-1432 MHz	2.4 GHz	402-405 MHz	2.4 GHz 868/915 MHz	many bands
Range	>100 m	0-100 m	0-10 m	0-10 m	2 m

Table 2.2: Frequency bands and range summary of WBAN wireless protocols [3, 2]

Narrowband PHY, Differential Binary Phase-shift Keying (DBPSK), Differential Quadrature Phase-shift Keying (DQPSK), and Differential 8-Phase-shift Keying (D8PSK) modulation techniques are used in all the above bands except the 420-450 MHz which utilizes Gaussian Minimum Shift Keying (GMSK) modulation [29]. On the other hand, Ultra Wideband PHY operates in the range 3.1-10.6 GHz with a low and high band. Each band is divided into numerous channels with a bandwidth of 499.2 MHz each, the low band with channels 1-3 and the high band with channels 4-11. Both channels 2 and 7 are mandatory channels with central frequencies, $f_c = 3993.6$ MHz and $f_c = 7987.2$ MHz, respectively. UWB compliant devices must support one of the two mandatory channels while having low computational complexity and low-power signals, with data rates in the range of 0.5-10 mbps [29]. While HBC PHY operates in two frequency bands: 16 MHz (US, Japan, Korea) and 27 MHz (US, Japan, Korea, Europe). HBC covers packet structure, modulation, preamble, etc of the protocol in WBANs [29]. Table 2.2 presents a summary of the bands and transmission range at which IEEE 802.15.6 and the wireless protocols presented in Appendix A operate in.

2.4 Spread Spectrum in WBANs

Given the challenges posed in WBANs as presented in Section 1.2, several MAC and physical layer protocols have been developed for collision avoidance in wireless networks,

including centralized and distributed channel access scheduling or multiple access techniques [31]. Of interest is the use of multiple-access protocols such as Time Division Multiple Access (TDMA), Frequency Division Multiple Access (FDMA) and Code Division Multiple Access (CDMA) which are widely used in conventional wireless voice and data networks [32]. For such multiple access schemes, the channel access is scheduled by time, frequency or coding respectively among users. However, the majority of the protocols used for cellular and classical wireless networks are unlikely to be directly applicable in on-body wireless sensor networks, as they require many actions to be taken by the battery-constrained sensor node. Besides circuit complexity and cost, some classical multiple access protocols impose more delay in data transmission. TDMA protocols, for instance, where users are granted channel access at unique allocated time slots, exhibit a poor bandwidth efficiency because of the long time delay in using the channel. Furthermore, this latency is undesirable for medical WBAN applications, where transmission of physiological signs of patients are vital. In addition, any TDMA-based scheme requires strict synchronization among various sensors which increases the circuit complexity and power requirement. FDMA, on the other hand, displays bandwidth inefficiency due to the splitting of the whole spectrum between users. Furthermore, wake up synchronized protocols used in the IEEE 802.11 standard [33] that use the DSSS technique may not be a suitable choice for WBAN, as they cannot meet the stringent energy efficiency requirements for WBANs. More precisely, since biosensors in WBANs operate in an asynchronous duty-cycling mechanism (as shown in Section 2.2.1), they have the advantages of low complexity in implementation and lower power consumption than the synchronous case.

Taking the above considerations into account and to provide feasible wireless links between the biosensors and the CCU in a body-centric wireless network, the following issues have to be addressed properly: *i*) avoid collision, *ii*) mitigate MAI caused by simultaneous transmission of multiple sensors, and *iii*) facilitate asynchronous transmission. Among

various multiple access techniques, Direct Sequence Code Division Multiple Access (DS-CDMA) scheme is the most promising physical layer and multiple access technique for on-body wireless networks, as it meets the following requirements: *i*) collision-free, *ii*) multi-path resilient properties, *iii*) robust against interference, *iv*) support various data rates, and *v*) uses available resources efficiently. In contrast to TDMA and FDMA techniques, the CDMA approach allows multiple sensors to transmit concurrently within the same time over a common frequency band. This results in achieving higher bandwidth efficiency and capacity than other multiple access techniques. In addition, on the contrary to synchronous protocols used in the IEEE 802.11 standard, the CDMA technique in an asynchronous WBAN enables the nodes to operate in an efficient energy manner by controlling the interference through choosing proper spreading codes.

2.5 Code Division Multiple Access in WBANs

For an asynchronous WBAN, where the transmission from various sensors is bursty over low duty-cycle, TDMA and FDMA schemes are not beneficial, as a certain percentage of the available time or frequency slots assigned to each node would be useless. More recently, the attention of the researchers has been drawn to using DS-CDMA in wireless sensor networking applications, where multiple sensors transmit data simultaneously to a central node using different spreading codes [34, 35, 36]. In [37], the authors propose a DS-CDMA with multi-carrier transmission in a WBAN for health monitoring. However, multi-carrier transmissions may not be suitable for energy constrained WBANs due to the high complexity and power consumptions imposed by the transceiver hardware.

It is shown that deploying MAI suppression techniques in DS-CDMA wireless applications can significantly improve the performance of the network such as the system capacity [38]. In [12], the authors present an interference mitigation technique to be employed in CDMA-based WBANs in which lowers the effect of MAI in such networks.

The authors assume a CDMA-based WBAN with m-sequences making up the spreading codes for each sensor node. M-sequences have minimal cross-correlation properties when compared to other spreading codes. The main contribution to the work in [12] is the proposed interference estimation technique using Fast Walsh-Hadamard Transform (FWHT), which estimates the interfering signal at the CCU, and subtracts it from the received signal (interference cancellation) to decode for the desired sensor. This approach allows the CCU to mitigate interference caused by both the asynchronous nature of WBANs and the non-orthogonal nature of m-sequences. This approach requires a slight increase in computation at the CCU but does not require further computation at the sensor node, which is ideal due to the power-constrained nature of sensor nodes. On the other hand, some work in the literature proposes time-hopping techniques for asynchronous WBANs in order to mitigate MAI. In [21], the authors consider transmitter only sensors in CDMA-based WBAN where no synchronization is achieved. By assigning time-hopping sequences to sensor nodes at which they can transmit their data over to the CCU, this ensures no collision occurs between the transmitting sensors and MAI is effectively avoided. This technique performs well, but since WBANs deal with vital physiological data, restricting sensor transmission time might be critical to patient monitoring.

2.5.1 Spreading Codes

In CDMA-based wireless sensor networks one can also control the effect of MAI by using semi-orthogonal spreading codes. Semi-orthogonal codes are spreading codes that produce near zero cross-correlation (refer to Section 3.2). In [39], the authors present a methodology to generate a set of orthogonal short codes that outperform traditional spreading codes used in sensor networks. The authors do not consider the asynchronicity of the WBAN at which would make the spreading codes lose their orthogonality and MAI would persist. In CDMA-based WBANs where synchronicity between the sensor nodes

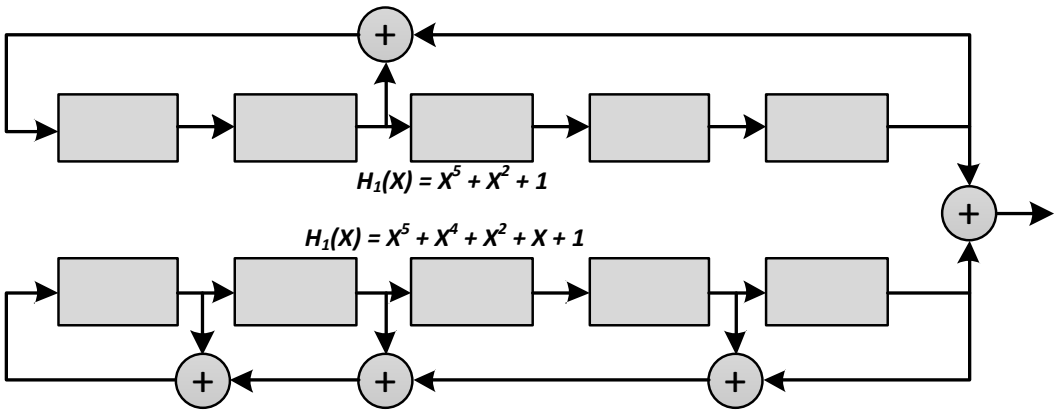

Figure 2.5: Example of Gold Code generator [5]

can be achieved, using orthogonal Walsh-Hadamard codes for spreading can effectively eliminate interference. Hadamard codes are orthogonal (i.e. have zero cross-correlation) in the zero phase. In WBANs where the sensor nodes are asynchronous, Hadamard codes lose their orthogonality property, and effectively introduces MAI at the CCU.

Other semi-orthogonal codes that have near-zero cross-correlation in all time shifts have been proposed to be utilized in CDMA-based sensor networks such as:

Gold Codes: Presented in [13], Gold codes are sets of $2^n - 1$ sequences typically used in CDMA communications. When Gold sequences are cross-correlated, the result is one of $\left\{-1, \left(2^{\frac{n+1}{2}} - 1\right), -\left(2^{\frac{n+1}{2}} + 1\right)\right\}$. Gold sequences are generated by computing the modulo-2 sum of the output of two m-stage shift registers with preferred polynomials as shown in Figure 2.5.

Chaotic Codes: In [14], the authors study the properties of chaos codes that can be used in a CDMA system. The chaos phenomenon is able to produce chaotic sequences with very low cross-correlation, and it is shown that it can outperform Gold codes and m-sequences [14]. The codes are generated in this fashion:

1. Given (2.1) representing the growth of population v from time n to time $n+1$ by the growth factor r:

$$v_{n+1} = rv_n(1 - v_n) \tag{2.1}$$

where $0 < v_n < 1$, and r takes values between 0 and 4, it is shown that as r approaches 4, the system is driven to chaotic behaviour [40].

2. To generate chaotic codes from (2.1), r is set to 3.99 and v_n is set to an arbitrary initial condition. Code bits are realized as follows:

$$c_n = +1 \quad , \quad v_n \geq 0.5$$
$$c_n = -1 \quad , \quad v_n < 0.5$$

2.5.2 Receiver Designs

Conventional WBAN receivers implement a Single User Detection (SUD) technique, where the signal for sensor $\mathcal{S}_i$, $i = 1, 2, \cdots, K$ is decoded assuming the conditions (spreading codes and data rate) of the interfering nodes $\mathcal{S}_j$, $j \neq i$ is not known at the receiver. This receiver design assumes that there cannot be a compensation technique used to mitigate the effect of non-orthogonal spreading codes on MAI. In the proposed contribution, Section 4.1.4 details the implementation of SUD receivers in CDMA-based WBANs. There also exists a number of Multiple User Detection (MUD) methodologies commonly used in wireless systems such as the decorrelating receiver, zero-forcing multiuser detector and the Minimum Mean Square Error (MMSE) receiver. Such receivers are implemented to mitigate MAI and Inter-Symbol-Interference (ISI) in DSSS systems that utilize non-orthogonal or semi-orthogonal codes for spreading. In [41], the authors study the effect of the decorrelating receiver in asynchronous and synchronous CDMA-based WBANs.

Decorrelating Receiver utilizes the information readily available at the CCU to mitigate MAI. Conveniently it is only practical at the CCU where the information about spreading codes $w_i, i = 1, 2, \cdots, K$ are readily available and there are less power consumption constraints. If $\mathbf{R}$ is defined as the $K \times K$ correlation matrix whose elements are:

$$\rho_{i,j}(k) = \int_{-\infty}^{\infty} w_i(t) w_j(t), \tag{2.2}$$

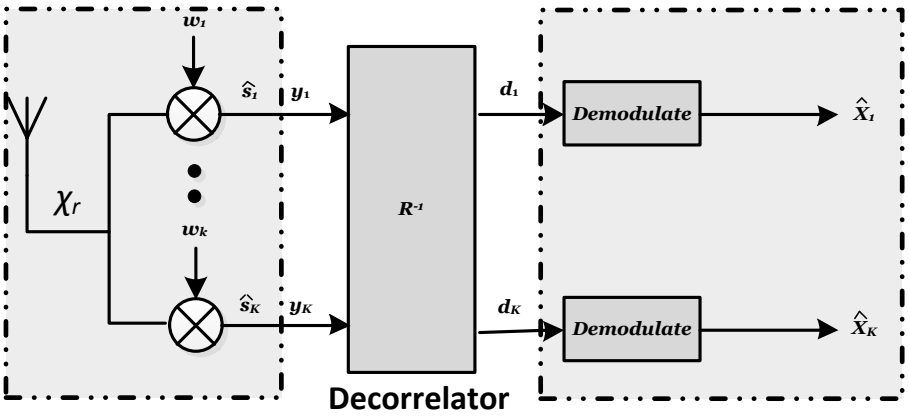

Figure 2.6: The Decorrelating Receiver in CDMA-based WBANs

where $i, j = 1, 2, \cdots, K$ and the vector $\mathbf{Y} = [y_1\ y_2\ \cdots\ y_K]$ represents the de-spread signals from users $i = 1, 2, \cdots, K$ as shown in Figure 2.6.

$$\mathbf{Y} = \mathbf{RS} + \mathbf{N}, \tag{2.3}$$

where $\mathbf{S} = [s_1\ s_2\ \cdots\ s_K]$ is the vector representation of the original signal s_i from sensor $\mathcal{S}_i$, and $\mathbf{N} = [n_1\ n_2\ \cdots\ n_K]$ is the corresponding AWGN for sensor $\mathcal{S}_i$ respectively. Hence in a decorrelating receiver the output vector $\mathbf{Y}$ is multiplied by $\mathbf{R}^{-1}$ to produce the following:

$$\mathbf{D} \quad = \quad \mathbf{RR}^{-1}\mathbf{S} + \mathbf{R}^{-1}\mathbf{N} \quad = \quad \mathbf{S} + \mathbf{R}^{-1}\mathbf{N} \tag{2.4}$$

where $\mathbf{D} = [d_1\ d_2\ \cdots\ d_K]$. This insures that the effect of non-orthogonality of the spreading codes is compensated for by the $\mathbf{R}^{-1}$. The obvious disadvantage here is that the noise will be enhanced by $\mathbf{R}^{-1}$.

It is evident in [41] that using MUD techniques at the receiver increases the overall performance of the system from a Bit-Error-Rate (BER) point of view.

2.6 Conclusions and Problem Definition

As presented in this chapter, the design of WBANs is such that it supports a variety of sensing devices that have: (i) multiple data rates, (ii) different duty cycling and timing mechanisms, and (iii) physiologically diverse data types (ECG, EEG, heart pulse). As the sensor nodes independently transmit their data to the CCU, they do so in an asynchronous fashion. As the sensor nodes utilize the same transmission bandwidth, they may interfere on each other and effectively cause packet collision at the CCU. Packet Collision causes transmitted data to be lost, and hence cannot be decoded correctly at the CCU. In the case where there is no feedback (bidirectional) channel between the sensor nodes and the CCU, the CCU cannot communicate back to the sensor node to re-send the lost packets. While in the case where a feedback channel is established, re-sending packets is considered to be a major energy waste in such power-constrained networks.

To combat the problem of the loss of orthogonality of spreading code, this work proposes the use of a special set of orthogonal codes extracted from the Walsh-Hadamard matrix, COWHC, that do not lose their orthogonality property due to the asynchronous nature of the WBAN. In addition, to address the challenges of asynchronicity in WBANs and spectrum utilization, the work presented in this study proposes the use of a CDMA-based WBAN that utilizes the COWHC for spreading. To the best of our knowledge and according to the simulation results presented in Section 3.5 and Section 4.2, the Cyclic Orthogonal Walsh-Hadamard Codes are capable of mitigating the effects of MAI in asynchronous CDMA-based WBANs while efficiently utilizing the allocated spectrum.

Chapter 3

Novel Cyclic Orthogonal Walsh-Hadamard Codes

This chapter investigates the first proposed contribution of this thesis document, the Cyclic Orthogonal Walsh-Hadamard Codes (COWHC). First, the theoretical and background details of COWHC is introduced. Next, a comprehensive overview of the validation methodology used in confirming the performance of the proposed contribution is provided. Then, simulation setup and results in support of the cyclic orthogonal spreading codes is presented. Finally, a summary of the contribution and finding presented in this chapter is provided.

3.1 Hadamard Codes in CDMA-based WBANs

In a CDMA-based body centric wireless sensor network where K on-body biosensors denoted by $\mathcal{S}_1, \mathcal{S}_2, \cdots, \mathcal{S}_K$ communicate to the CCU simultaneously and over a common spectrum, orthogonal spreading codes are assigned to the sensor nodes in a fashion that minimizes MAI. At the sensor nodes, the modulated signal s_i, $i = 1, 2, \cdots, K$ is directly multiplied by a pseudorandom spreading sequence w_i with chip duration T_c and processing gain $N \triangleq \frac{T_b}{T_c}$. The length of the pseudorandom spreading sequence is a function of

different parameters such as the number of on-body biosensors, the available spectrum, and the targeted performance of the network. The received signal at the CCU is given by:

$$\mathcal{X}_r = \sum_{i=1}^{K} w_i s_i + \eta, \tag{3.1}$$

where w_i, $i = 1, 2, \cdots, K$ are unique pseudorandom spreading codes, and η is Additive White Gaussian Noise (AWGN).

Walsh-Hadamard codes constitutes a set of orthogonal codes that have received attention in communication and signal processing applications and have been widely used in DS-CDMA communications. Inherently the codes generated from the Walsh-Hadamard Matrix $\mathbf{H}_{2^k}$ are orthogonal in the zero-phase (i.e. there exists no mutual shift). The utilization of Hadamard codes to constitute w_i, $i = 1, 2, \cdots, K$ is particularly useful in synchronous CDMA-based WBANs where biosensors in the network can achieve perfect time synchronization. In WBANs where perfect synchronization in time is not possible the use of Walsh-Hadamard codes as spreading codes will introduce MAI. The asynchronous nature of WABNs will make the Hadamard codes lose their orthogonality as they are mutually shifted in time.

The Walsh-Hadamard matrix $\mathbf{H}_{2^k}$ is a special matrix of size 2^kx2^k. Given

$$\mathbf{H}_1 = [1] \quad , \quad \mathbf{H}_2 = \begin{bmatrix} 1 & 1 \\ 1 & -1 \end{bmatrix} \tag{3.2}$$

a higher dimensional Hadamard matrix $\mathbf{H}_{2^k}, k > 1$ is produced as follows:

$$\mathbf{H}_{2^k} = \begin{bmatrix} \mathbf{H}_{2^{k-1}} & \mathbf{H}_{2^{k-1}} \\ \mathbf{H}_{2^{k-1}} & -\mathbf{H}_{2^{k-1}} \end{bmatrix} = \mathbf{H}_2 \otimes \mathbf{H}_{2^{k-1}} \tag{3.3}$$

where $\otimes$ denotes the Kronecker product [42].

The rows in each of the Hadamard matrices generated above are mutually orthogonal to each other. One can test for orthogonality of the code using one of two methods:

i. Agreements and disagreements match: For example if w_1 represents the first row of $\mathbf{H}_{2^2}$ and w_2 the second row of the same matrix, such as:

$$w_1 = \begin{bmatrix} 1 & 1 & 1 & 1 \end{bmatrix}, w_2 = \begin{bmatrix} 1 & -1 & 1 & -1 \end{bmatrix}$$

It is evident that there are 2 agreements and 2 disagreements between w_1 and w_2. This property guarantees that the codes of w_1 and w_2 are orthogonal. The rows of $\mathbf{H}_{2^k}$ all mutually follow this property at the zero-phase.

ii. The cross correlation of w_1 and w_2 is equal to zero in the zero-phase. In fact, if:

$$w_1 = \begin{bmatrix} x_1, x_2, ..., x_{2^k} \end{bmatrix}, w_2 = \begin{bmatrix} y_1, y_2, ..., y_{2^k} \end{bmatrix}$$

then the cross correlation of w_1 and w_2 in the zero-phase is given as follows:

$$R_{w_1 w_2} = \sum_{l=1}^{2^k} w_1(l) w_2(l) = 0 \tag{3.4}$$

this property applies to all w_i, w_j, $i \neq j$.

The orthogonality property of the Walsh-Hadamard codes is lost if the codes are phase shifted. Shifted codes when cross-correlated using (3.4) result in a non-zero cross-correlation value. If Hadamard codes are used to spread the sensor nodes in an asynchronous WBAN, their non-orthogonality will introduce MAI at the CCU.

3.2 Cyclic Orthogonality of Hadamard Codes

To combat the asynchronicity problem in CDMA-based WBANs, this section investigates the proposed use of a special set of Hadamard codes extracted from the $\mathbf{H}_{2^k}$ matrix that are orthogonal to each other at every phase shift ϕ, where $\phi = 0, 1, 2, \cdots, 2^k - 1$ [43, 44].

If $\mathbf{W}(2^k, k)$ denotes the set of 2^k codes generated from the $\mathbf{H}_{2^k}$ matrix, $k \geq 1$, then the cross-correlation for codes w_i and w_j, $i \neq j$, at phase-shift ϕ is defined as follows:

$$R_{w_i w_j}(\phi) = \sum_{l=1}^{2^k} w_i(l) w_j(l+\phi), \tag{3.5}$$

All Hadamard codes are mutually orthogonal in the zero phase ($\phi = 0$) but some codes lose their orthogonality when $\phi \geq 0$. In [43] and [44], the authors show that one can extract $K = k + 1$ codes from the Hadamard matrix $\mathbf{H}_{2^k}$ that exhibit zero cross-correlation for all $\phi = 0, 1, 2, \cdots, 2^k - 1$. This set of K cyclically orthogonal spreading codes is called *Cyclic Orthogonal Walsh-Hadamard Codes* (COWHC). If COWHC are utilized for spreading in CDMA-based WBANs, then at the CCU where:

$$\hat{s}_i = w_i \mathcal{X}_r = {w_i}^2 s_i + \sum_{\substack{j=1 \\ j \neq i}}^{K} w_i w_j s_j + w_i \eta, \tag{3.6}$$

is the decoded signal for sensor $\mathcal{S}_i$, ${w_i}^2$ will equal to 1, and $w_i w_j$ will evaluate to zero due to their cyclic orthogonality. Hence the decoded signal for sensor $\mathcal{S}_i$ would equate to $\hat{s}_i = s_i + w_i \eta$, where the signals s_j, $j \neq i$, do not interfere on the desired signal s_i.

In order to validate the results presented in [43] and [44] the cross-correlation properties of the set of Hadamard codes generated from $\mathbf{H}_{2^k}$ is examined. If $\mathbf{W}(8, 3)$, the set of Hadamard codes extracted from $\mathbf{H}_8$ is used for illustration purposes, one can compute the mutual cross-correlation of all w_i, $i = 1, 2, \cdots, 8$ with each other as per (3.5) for all $\phi = 0, 1, 2, \cdots, 7$. It is observed in Figure 3.1 that the cross-correlation between the codes of $\mathbf{W}(8, 3)$ at the zero-phase are all zero as expected. However, in the first and second phases it is evident that only "some" codes exhibit zero cross-correlation; It is of particular interest to study these codes. When examined, one can find a unique set of $K = k + 1 = 4$ codes from the $\mathbf{W}(8, 3)$ that have zero cross-correlation in all phases $\phi = 0, 1, 2, \cdots, 7$. Lets denote w_i, as the code extracted from the $i^{th}, i = 1, 2, \cdots, 8$ row of $\mathbf{W}(8, 3)$. By inspection, a possible COWHC set is generated from:

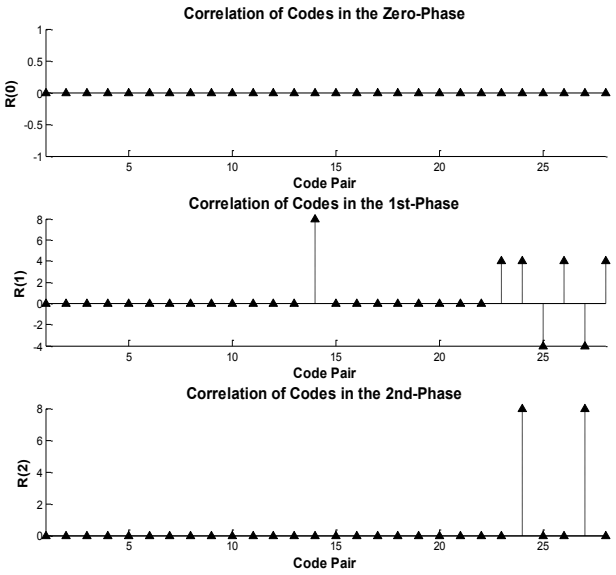

Figure 3.1: Cross correlation of $W(8,3)$ at the (a) zero, (b) 1st, and (c) 2nd phase

$$
\begin{aligned}
w_1 &= (1 \ , 1 \ , 1 \ , 1 \ , 1 \ , 1 \ , 1 \ , 1 \ ) \\
w_2 &= (1 \ , -1 \ , 1 \ , -1 \ , 1 \ , -1 \ , 1 \ , -1 \ ) \\
w_4 &= (1 \ , -1 \ , -1 \ , 1 \ , 1 \ , -1 \ , -1 \ , 1 \ ) \\
w_5 &= (1 \ , 1 \ , 1 \ , 1 \ , -1 \ , -1 \ , -1 \ , -1 \ )
\end{aligned}
$$

this makes up one possible set of cyclically orthogonal codes extracted from the $\mathbf{H}_8$ that can be used to spread 4 sensor nodes in the proposed CDMA-based WBAN. Inherently if w_i, $i = 1, 2, 4, 5$ are used for spreading the sensor nodes in CDMA-based WBAN then one can ultimately eliminate the contribution of the interfering signals and produce a decoded message $\hat{s}_i = s_i + w_i\eta$ that contains only the desired s_i and AWGN.

3.2.1 COWHC selection

As per the work presented in [44], the following technique is used to randomly select a subset of cyclically orthogonal codes from the Hadamard matrix. Given the Hadamard matrix $\mathbf{H}_{2^k}$ with dimension $D = 2^k$, it is shown in [44] that if $\mathcal{H}_i$ is the i^{th} row of $\mathbf{H}_{2^k}$

then one can divide $\mathbf{H}_{2^k}$ into the following subsets:

$$\{\mathcal{H}_i\}_{i\in\mathcal{C}} \quad , \quad where \;\; \mathcal{C} = \left\{\bigcup_{l=1}^{k} \mathcal{C}_l\right\} \bigcup \{1\} \tag{3.7}$$

and $\mathcal{C}_l = \left\{2^{k-l}+1, \cdots, 2^{k-l+1}\right\}$. Given the subsets in (3.7), one can define a COWHC set of K codes by selecting a single code from each subset. If $\mathbf{H}_{2^4}$ is used for illustration purposes, then given (3.7) the following subsets are generated:

$$\{1\} \;,\; \mathcal{C}_1 = \{2\} \;,\; \mathcal{C}_2 = \{3,4\} \;,\; \mathcal{C}_3 = \{5, \cdots, 8\} \;,\; \mathcal{C}_4 = \{9, \cdots, 16\}$$

and hence a COWHC set of size $K = 5$ can be utilized for spreading by selecting a single code (row) from each of the above subsets (i.e. w_1, w_2, w_4, w_7, and w_{11}).

3.3 Validation Methodology

This section discusses the methodological approach to validating the proposed contributions. The application in hand is asynchronous CDMA-based WBAN where MAI can produce packet collision when multiple biosensors wirelessly and simultaneously communicate to the CCU. The proposed COWHC spreading sets can reduce the effect of MAI in such networks due to their cyclic orthogonality and effectively boost the reliability of data transmission. Hence, the aim in simulations is to achieve the following:

1. Validate the performance of COWHC spreading sets in the proposed CDMA-based WBAN (Chapter 4) and compare the results to other spreading codes used in existing solutions.

2. Identify an ideal and complete communication system to foster COWHC while maintaining better performance than that available in the literature.

3. Identify a complete list of the advantages and limitations of the proposed contributions, and ways to expand and further modify the presented work in the future.

3.3.1 Validation Metric

In a communication system, there exists a large set of design and testing metrics both at the PHY and MAC layers. In the attempt to validate the proposed work, it is crucial to select a study and comparison metric that is fitting to the application in hand. The core problem to this project is the packet loss that occurs due to MAI in wireless medical networks. Of interest are medical devices that are placed on-body or implanted in the human body, both of which have relatively low data rates as shown in Table 2.1, this makes the quality of transmission very sensitive to packet-loss.. The goal is to maximize the reliability of the data transmission in the proposed WBAN, and in medical devices reliability depends on the data rates [1]. Hence as a comparison and testing metric, Bit-Error-Rate (BER) is selected as the primary testing metric. The BER helps better understand the nature of the reliability of transmission at the bit level of the proposed WBAN and how the simulated system is capable of eliminating packet loss.

The BER is a measure of the ratio between the number of error bits in the decoded message compared to the total number of bits in the original message. It provides an estimation of the bit error probability of the transmission. BER is generally used as a test metric where transmission reliability is being examined [41] . In the scope of the project, only BER is used to examine the performance of the proposed system. As shown in Section 3.5 and Section 4.2, the BER will be used to quantify the transmission reliability with multiple noise levels. BER will be shown in the log scale, and Signal-to-Noise-Ratio (SNR) as decibels (dB). To further strengthen the results in the future, the performance of the contributions could be studied from the network throughput, capacity, power and energy points of view.

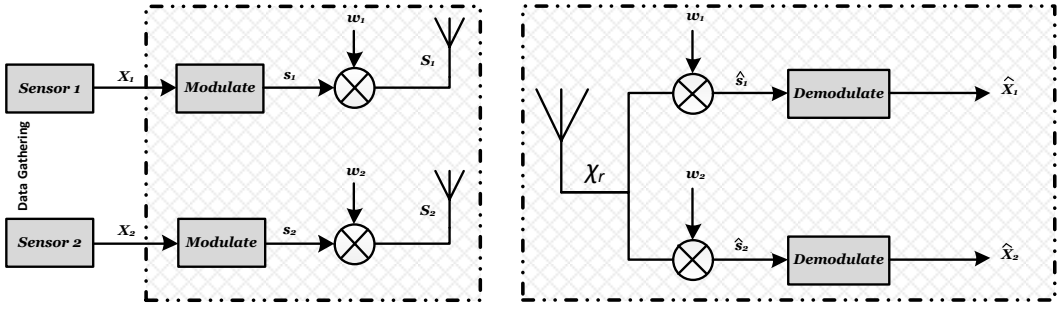

Figure 3.2: CDMA-based communication system for WBANs with two sensor nodes

3.3.2 Approach to Performance Validation

To show the validity, extent and limitation of the work presented in this thesis document, the following two scenarios are qualitatively and analytically studied, namely:

1. **Simple Network Scenario**

2. **Ideal Network Scenario**

3.3.2.1 Simple Network Scenario

The smallest WBAN is composed of a minimum of two sensor nodes. Testing a network with only two sensor nodes allows for the validation of the proposed contributions under practical conditions while maintaining low computational complexity. It also insures that there could only be one interfering signal, ultimately decoding for the desired signal is easier as there exists minimal interference. Figure 3.2 illustrates a WBAN system with the two sensors $\mathcal{S}_1$ and $\mathcal{S}_2$ transmitting periodically and over the same frequency band to the CCU.

The digitized physiological signals X_1 and X_2 are modulated at the transmitter by a predefined modulation technique to produce the modulated signals s_1 and s_2 respectively. Each sensor node is assigned a unique spreading code w_1 and w_2 respectively, that are

known at the CCU. The spread signals are then transmitted in an AWGN channel with Rayleigh flat-fading. The signal $\mathcal{X}_r$ received at the CCU is:

$$\mathcal{X}_r = w_1 s_1 + w_2 s_2 + \eta, \tag{3.8}$$

where η is AWGN for a given SNR. If the desired signal is s_1, the received signal $\mathcal{X}_r$ is multiplied with the corresponding spreading code for sensor $\mathcal{S}_1$, w_1. This produces a decoded signal as follows:

$$\hat{s}_1 = w_1 \mathcal{X}_r = w_1 \times (w_1 s_1 + w_2 s_2 + \eta) = {w_1}^2 s_1 + w_1 w_2 s_2 + w_1 \eta \tag{3.9}$$

Hence if the proposed COWHC are used for spreading the two sensors, (3.9) will equate to $\hat{s}_1 = s_i + w_1 \eta$. Ultimately eliminating the interference sensor $\mathcal{S}_2$ poses on sensor $\mathcal{S}_1$. Table 3.1 summarizes the environmental parameters that govern a simple WBAN with two sensor nodes. It is worth noting that since there only exists two sensors in the network, common practice in literature studies to decrease the spreading factor accordingly with the number of users. In this scenario, the simulation will assume a practical scenario where the 'default' parameters shown in Table 3.1 are fixed for both the simple network scenario and the ideal network scenario (Section 3.3.2.2). This is done such that the simulation assumes a practical design rather than an experimentation design, where in practice the spreading factor will not be changed as the number of active sensors change in the network.

3.3.2.2 Ideal Network Scenario

While the objective of the presented work aims at enhancing the overall performance of WBANs, one must keep the patients well being as well as comfort in mind. Hence, in WBANs the total number of sensors worn by the patient must be very low such that the patients' comfort is not compromised [16]. After studying and analyzing the performance

Table 3.1: Environmental Parameters for Simple Network Scenario

Parameter	Description	Range/ Type	Why?
Number of sensors	The total number of sensors simultaneously transmitting in WBAN	2	To validate our proposed work with the simplest network structure
Spreading Factor (N)	$\frac{T_b}{T_c}$, also called *Processing Gain*	32 and 64	Maintain practical limit on number of users while keeping minimal bandwidth requirement
Signal-to-Noise Ratio (SNR)	The power ratio of the transmitted signal to AWGN in the channel	-10dB to 20dB	Test the operational capacity of the proposed design under a large range of practical channel noise
Receiver Design	Type of receiver used for decoding at the CCU	Conventional (SUD) and Decorrelating Receiver (MUD)	Analyze the performance gain/ loss when different receiver designs are utilized at the CCU
Channel Fading	The statistical model used to simulate a practical operational environment	Rayleigh Flat-fading	Use a simple channel model that closely correlates to the real operational environment of the proposed WBAN
Spreading Codes	The type of orthogonal/ semi-orthogonal codes used to spread the sensor nodes	COWHC, non-cyclic Hadamard Codes, Gold codes and Chaotic codes	Test the performance gain/ loss of the proposed codes to those used in prior art

of a simple network in Section 3.3.2.1, next is studying a network that can support 6 sensors placed on the users body. The number 6 was chosen such that (i) the designed WBAN does not interfere with the comfort of the user [16], and (ii) it is the largest possible $K = k + 1$ for the lowest spreading factor $N = 32$ proposed for use in Table 3.1. The sensors communicate to the CCU in the same fashion as shown in Section 3.3.2.1 and Figure 3.2. Ultimately the transmitted signal $\mathcal{X}_r$ will be as follows:

$$\mathcal{X}_r = \sum_{i=1}^{6} w_i s_i + \eta, \tag{3.10}$$

where η is AWGN for a given SNR. Then the decoded signal for sensor $\mathcal{S}_1$ is:

$$\hat{s}_1 = w_1 \mathcal{X}_r = w_1 \times \left(w_1 s_i + \sum_{i=2}^{6} w_i s_i + \eta \right) = {w_1}^2 s_i + \sum_{i=2}^{6} w_1 w_2 s_2 + w_1 \eta \tag{3.11}$$

which equates to $\hat{s}_1 = s_i + w_1 \eta$ if COWHC $w_i, i = 1, 2, \cdots, 6$ are used for spreading. The environmental parameters are the same as those presented in Table 3.1 with the exception shown in Table 3.2:

Table 3.2: Environmental Parameters for Ideal Network Scenario

Parameter	**Description**	**Range/ Type**	**Why?**
Number of sensors	The total number of sensors simultaneously transmitting in WBAN	6	To examine the network performance when more sensor nodes are available

3.4 Simulation Setup

Table 3.3: List of Simulation Parameters

Name	**Description**	**Simulation Range**
Num_Users	Total number of users in the network	1 - 7 (larger for non-COWHC)
dataLen	Number of bits in each cycle (over T_N)	1 - 100 kb
ittTimes	Number of cycles	1 - inf
N	Spreading factor	8 - 128
SNRall	SNR operating range (dB)	-20 - 20
CodeType	Type of spreading codes to be used	'cyclicwalsh', 'noncyclicwalsh', 'gold', 'chaotic'
RecType	Receiver type	'conventional', 'decorrelator'
Fading	Rayleigh flat-fading	'1' = Yes, '0' = No
ModType	Type of modulation	'bpsk', 'qpsk', 'oqpsk', 'pi2dbpsk', 'pi4dqpsk'

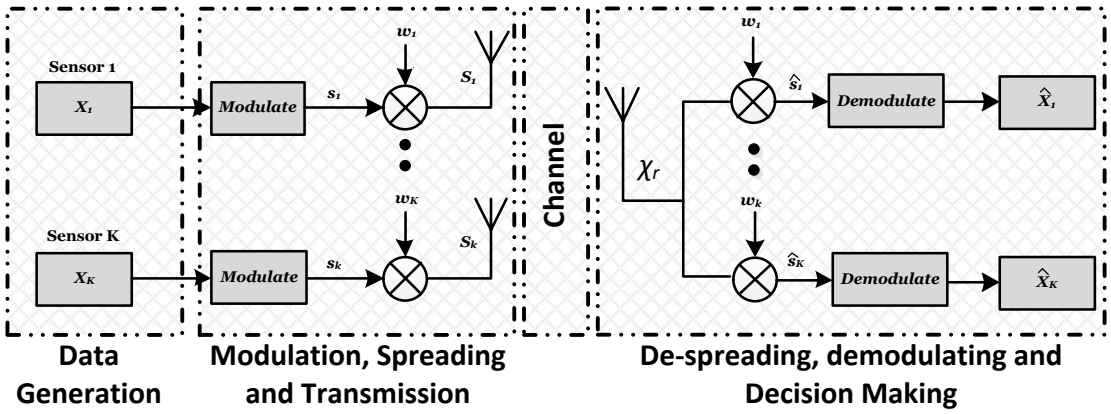

Figure 3.3: System design of the CDMA WBAN Simulation Model

The simulation model was developed entirely in MATLAB in an object oriented style and as visualized in Figure 3.3. Presented in Figure 3.4 is the program flow where in the initiation stage, the simulation parameters are first defined as per Table 3.3 and spreading codes are generated for spreading the different sensor nodes in the WBAN. The simulation program is designed to iterate over thousands of duty cycles, and for each iteration the data generation, transmission, reception and decoding is computed for the entire network. Each iteration represents one cycle, T_N, as shown in Figure 2.3 where raw binary message data is first generated for all sensors in the network, and then modulated using the user-defined modulation scheme. Next, spreading, transmission, and receiving is simulated over a nested loop that iterates over the user-defined SNR range. This nested loop examines how the network behaves under different AWGN noise levels. Finally once decoding is completed, the decoded signal is compared to the original signal by calculating the BER.

Below are details pertaining the multiple stages of the simulation setup:

Spreading Code Generation:

- **COWHC**: the number of codes produced from the Hadamard matrix $\mathbf{H}_{2^k}$ where $N = 2^k$ is the spreading factor, is $K = k + 1$. Hence, one can only generate a max-

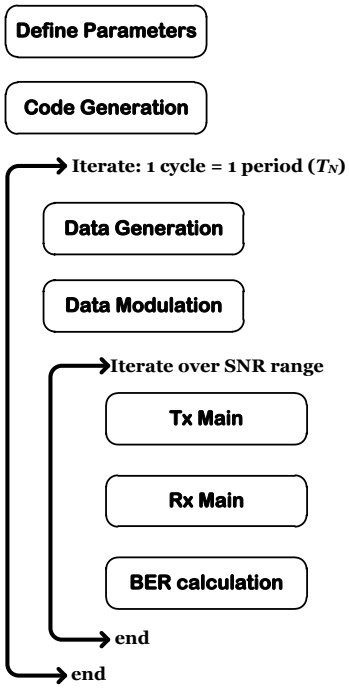

Figure 3.4: Program and command flow in simulation package

imum of $K = log_2(N)$ codes, where $K \geq Num\_Users$. The MATLAB program implements the selection technique detailed in Section 3.2.1 such that it randomly selects a code from different subset for a total of K codes. The K cyclically orthogonal codes are then randomly assigned to sensors $\mathcal{S}_i$, $i = 1, 2, \cdots, Num\_Users$. There exists no unique code distribution algorithm as all the produced codes behave in similar fashion.

On the contrary, if codes from the same subset are selected as presented in Section 3.2.1, a set of Hadamard codes that are only orthogonal to each other in the zero-phase are extracted. By doing so, the set of "noncyclic" Hadamard codes are used to qualitatively compare the performance to their cyclic counterparts.

- **Gold and chaotic codes:** a Gold sequence generator was used to implement the PN sequence generator shown in Figure 2.5. The simulation program randomly generates and assigns K codes of size $N = 32$ and $N = 64$ using the following

preferred polynomials:

N = 32

$$H_1(X) = X^5 + X^2 + 1$$
$$H_2(X) = X^5 + X^4 + X^2 + X + 1$$

N = 64

$$H_1(X) = X^6 + X + 1$$
$$H_2(X) = X^6 + X^5 + X^2 + X + 1$$

On the other hand, and as per the material presented in Section 2.5.1, the simulation package also generates chaotic codes in order to compare the performance to that of the proposed COWHC codes. The program generates K chaotic codes of length $N = 32$ and $N = 64$ in the fashion presented in Section 2.5.1.

Data Gathering: existing WBAN devices use digital sensors to measure the intended physiological signal. As shown in Table 2.1, typical WBAN sensors have a variety of data rates. For all practical purposes and to keep low system level complexity, in the simulation it is assumed that all sensors have the same data rate. As discussed in Section 2.6, the wide range of data rates existent in WBANs primarily contribute to asynchronicity in the network, hence in the simulation package asynchronicity is manually introduced to the biosensors as shown in Figure 3.6. Raw sensor signals are generated using a random sequence generator in MATLAB. These binary signals represent the raw message signal acquired at the sensor nodes. Hence for each cycle X_i, $i = 1, 2, \cdots, Num\_Users$ signals of size "dataLen x M" are produced, where M is the modulation constellation size. This ensures that after modulation, s_i, $i = 1, 2, \cdots, Num\_Users$ is of size "dataLen". $Note$: this ensures that the data rate for quadrature modulation (i.e. QPSK) is double than that of binary modulation (i.e. BPSK) while maintaining the same transmission bandwidth.

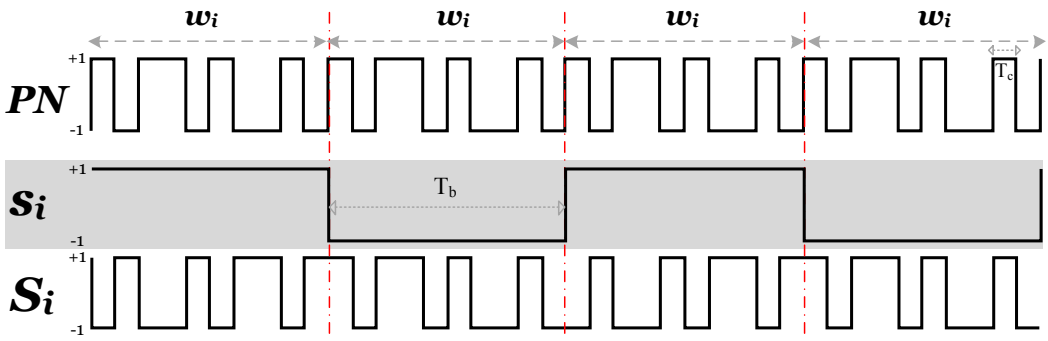

Figure 3.5: Overview of signal spreading in CDMA

Modulation, spreading and transmission methodologies: sensor data is next modulated using the pre-defined modulation technique. The binary sensor data in x_i is mapped into its complex equivalent (refer to Appendix B) to produce s_i. Next, after assigning the spreading codes w_i, $i = 1, 2, \cdots, Num\_Users$ to all users, s_i is spread with its corresponding spreading code. The essence of spreading in CDMA is shown in Figure 3.5, where each s_i bit is multiplied with the w_i code.

Finally the spread sensor signals are manually desynchronized in the following fashion:

1. All sensors have the same active mode duration T_{ac} (refer to Section 2.2.1).

2. Each sensor will be active and transmitting for a total of T_{ac} seconds every $2 \times T_{ac}$ seconds.

3. Sensors are unaware of each others activity modes.

the above asynchronicity mechanism can be visualized in Figure 3.6.

Channel model: the program simulates a Rayleigh flat-fading AWGN channel. The analytical detail of the channel environment is presented in Section 4.1.3. In the simulation package, the channel fading coefficients h_i, $i = 1, 2, \cdots, Num\_Users$ is generated as follows:

$$h_i = \frac{1}{\sqrt{2}} (P + iQ)$$

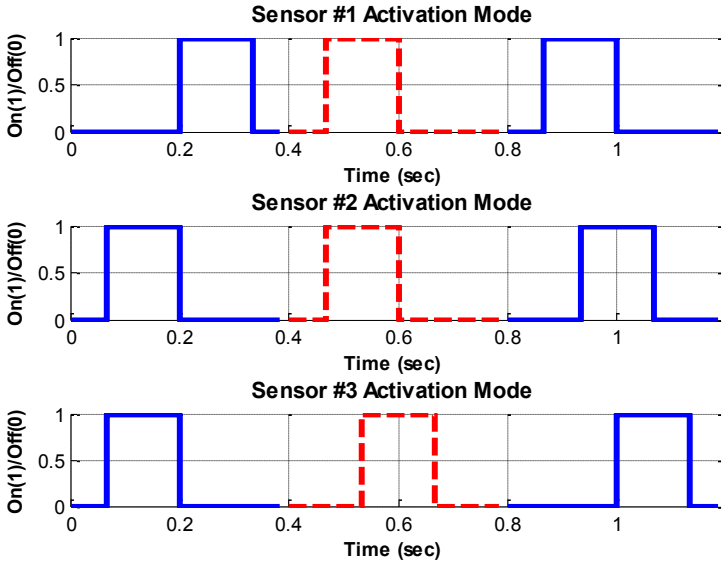

Figure 3.6: An asynchronous duty-cycling process in a practical WBAN

where $P, Q \sim \mathcal{N}(0,1)$. Given the flat-fading nature of the channel, h_i will be constant over one cycle (i.e. T_{ac}). On the other hand, AWGN $\eta_{i,l}$, is computed as follows:

$$\eta_{i,l} = \frac{\mathcal{P}_n}{\sqrt{2}} (P + iQ)$$

where $P, Q \sim \mathcal{N}(0,1)$, and $\mathcal{P}_n = \frac{1}{10^{\frac{SNR_{dB}}{10}}}$.

CCU: it is assumed that the CCU achieves perfect synchronization with the sensor nodes as the design and implementation of synchronization algorithms is beyond the scope of this project. In order to study the performance from the BER point of view and minimize the effect of channel statistics on the overall transmission, it is also assumed that the system implements coherent detection, where the channel model and statistics (i.e. h_i) are known at the receiver. To decode the signal from sensor $\mathcal{S}_i$, the effect of the channel fading is first eliminated from the received signal $\mathcal{X}_r$ by dividing by h_i. This will ensure that the received signal only contains the desired signal component and AWGN. Given that the CCU is aware of the spreading codes assigned to each sensor node, the complex signal is then de-spread with the corresponding w_i, and downsampled

by computing the mean over T_b. Finally, the complex signal is de-modulated, and the decoded message $\hat{\mathcal{X}}_i$ is realized. This binary message represents the raw sensor signal $\mathcal{X}_i$ generated at the node.

3.5 Simulation Results

3.5.1 Performance Results for Simple Network

In this simulation the aim is to examine the performance of the proposed COWHC spreading codes and compare it to conventional spreading codes such as Hadamard codes, Gold codes and chaotic codes. First, the performance is analyzed in a simple network scenario that is composed of 2 biosensors as described in Section 3.3.2.1. Table 3.4 summarizes the simulation parameters for this scenario.

Table 3.4: Simulation parameters used for simulating spreading codes in WBANs

Parameter	Range/ Type	Description
Num_Users	2 and 6	For simple and idea network designs
N	32 and 64	Common spreading factor range used in telecommunication (i.e. IS-95)
SNR	-10dB to 20dB	Practical channel noise operational range in WBANs
dataLen	1000	1kb/T_N
ittTimes	3000	Iterate over 3000 duty-cycles for accurate estimation
CodeType	'cyclicwalsh', 'noncyclicwalsh', 'gold', and 'chaotic'	Examine the behaviour of proposed and conventional spreading codes
RecType	'conventional'	Study a receiver design with conventional SUD
Fading	'yes'	Simulate a Rayleigh flat-fading channel
ModType	BPSK	Simple and highly efficient modulation scheme

Simulation objective and details: study the effect of COWHC spreading sequences in asynchronous CDMA-based WBAN with two sensor node (one desired and one interfering), and compare the performance to that of conventional spreading codes.

In this simulation, BPSK modulation is used as it is shown to be the most robust PSK modulation technique since it takes the highest level of noise to decode for the binary message (refer to Appendix B). This simple network design also implements a conventional SUD receiver and a Rayleigh flat-fading channel.

BER Performance: in Figure 3.7 the SNR vs BER performance is visualized for the four spreading codes with spreading factor N=32, while in Figure 3.8 spreading factor N=64 is used.

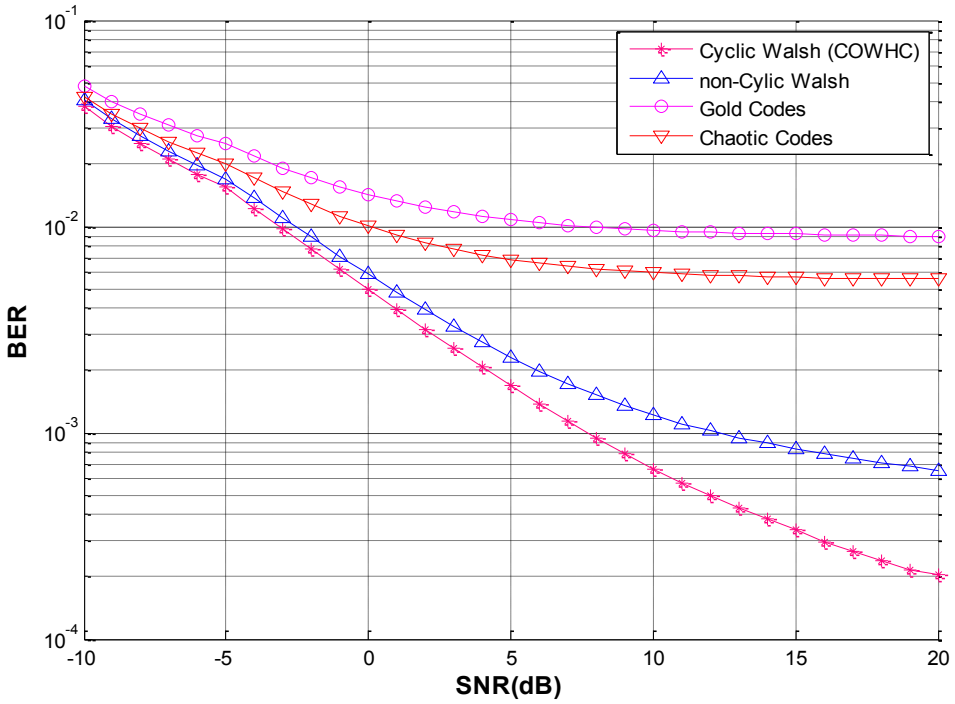

Figure 3.7: SNR vs BER performance results for multiple spreading codes in a simple 2-user WBAN with spreading factor N=32

Performance analysis: in the N=32 case (Figure 3.7), the COWHC spreading sequences achieve a tangible performance gain over the other spreading across the SNR range. Of interest is the performance at higher SNR ranges, where the signal power

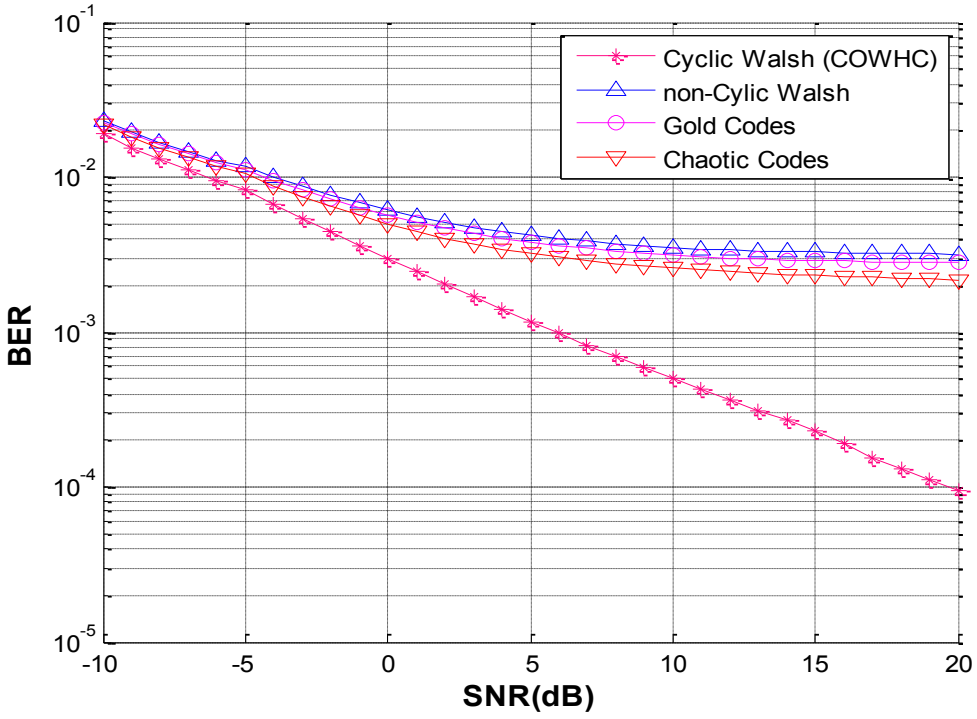

Figure 3.8: SNR vs BER performance results for multiple spreading codes in a simple 2-user WBAN with spreading factor N=64

is now much higher than the noise power. It can be visualized that Gold and chaotic codes have an error floor at $BER = 10^{-2.05}$ and $BER = 10^{-2.3}$ respectively, which is marginally higher than that of COWHC. Given the zero-cross correlation of COWHC codes, it is evident that COWHC mitigates the effect of MAI in a better fashion than Hadamard codes (as shown in Section 3.2). A similar scenario is realized in Figure 3.8 with N=64 where COWHC achieves the best BER performance with BPSK modulation and a conventional SUD receiver. Also when comparing Figure 3.7 to Figure 3.8, it is evident that spreading factor of N=64 performs better than N=32. The performance gain of N=64 over N=32 is justified since MAI is Gaussian distributed due to the central limit theorem, and hence the higher the spreading code the better the performance [45].

3.5.2 Performance Results for Ideal Network

Next, the performance of the proposed COWHC spreading codes are examined and compared to conventional spreading codes in an ideal network scenario that is composed of 6 biosensors as described in Section 3.3.2.2. The simulation parameters are similar to those of Table 3.4 with the only exception being the number of users (6 in this simulation).

Simulation objective: identify the effect of MAI on the spreading code design when more interfering signals are existent in the network.

BER Performance: in Figure 3.9 the SNR vs BER performance is visualized for the four spreading codes with spreading factor N=32, while in Figure 3.10 spreading factor N=64 is used.

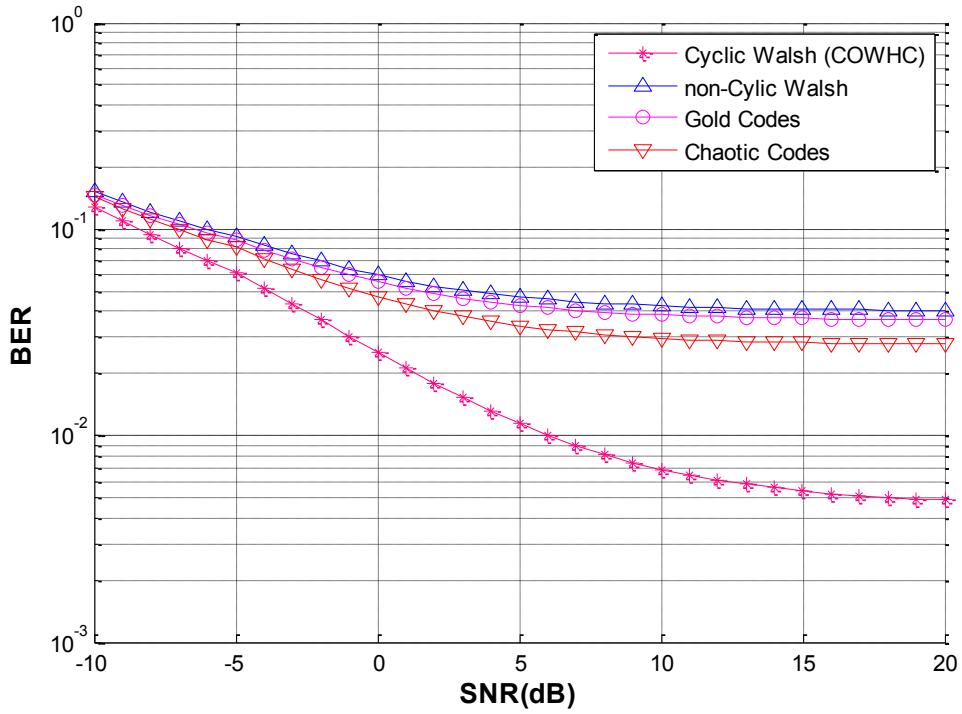

Figure 3.9: SNR vs BER performance results for multiple spreading codes in an ideal 6-user WBAN with spreading factor N=32

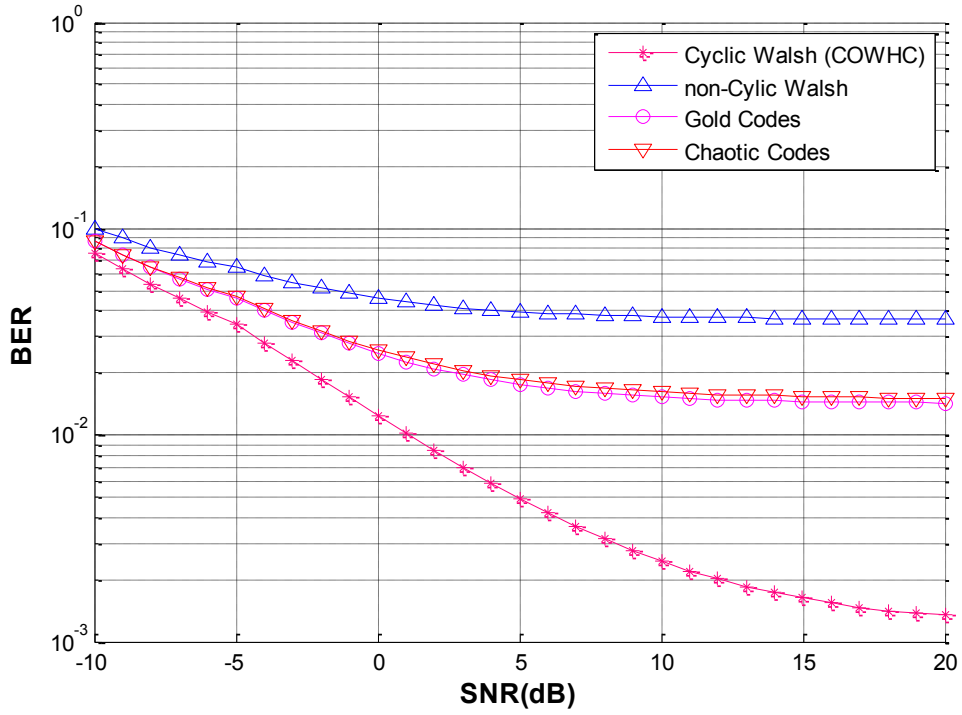

Figure 3.10: SNR vs BER performance results for multiple spreading codes in an ideal 6-user WBAN with spreading factor N=64

Performance analysis: similar to the results identified in Section 3.5.1, one can visualize that COWHC outperforms conventional spreading codes even when more interference exists in the network. As shown in Figure 3.9 and Figure 3.10, conventional spreading codes have an error floor at around $BER = 10^{-1.821}$ for SNR ranges above 5dB, while COWHC achieves a BER of $10^{-2.872}$ at 20dB. It is evident that even when more interference exists in the network, the cyclic-orthogonality of the COWHC mitigates MAI in a more efficient way and helps decrease the effect of interference on the decoding process.

It is worth mentioning that the performance in the ideal network scenario is is decreased than that of the simple network. In theory it is expected that the cyclic orthogo-

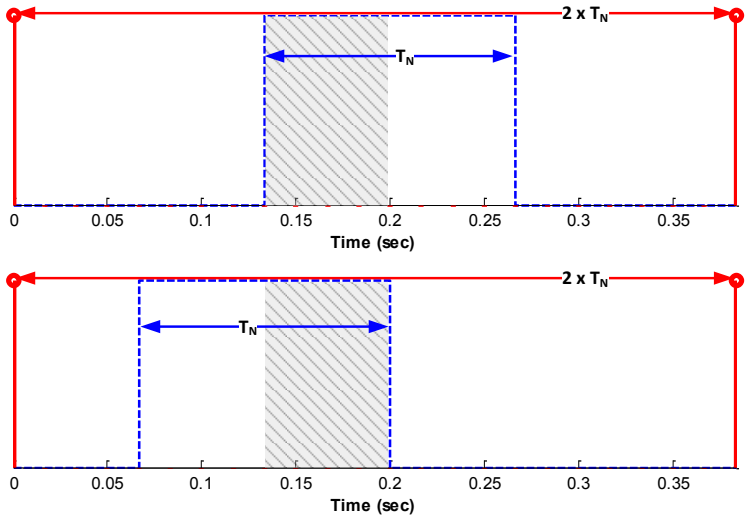

Figure 3.11: The correlation between asynchronous codes in a practical setup (only the shaded is correlated)

nality of the spreading codes completely eliminate the MAI, however after investigation, it is noticed that this decrease is due to the nature of asynchronicity in a practical setup. As shown in Figure 3.11, the simulated asynchronicity assumes a practical shift in time amongst the sensors (and effectively the codes), while in theory the property of cyclic orthogonality assumes a cyclic shift between the codes. This shift in time produces a very small residual correlation amongst the codes, and hence when the number of users is increased to the ideal scenario the effect of the interfering correlation residual is visualized in the BER performance. The produced residual is still significantly lower than that produced for Hadamard, chaotic and Gold codes. To study the effect of the correlation created in the practical asynchronous scenario, the L2-norm of the correlation matrix $\mathbf{R}$ whose elements are defined by (2.2), of 6 COWHC, Hadamard and Gold codes is computed. The norm is computed for $\mathbf{R}$ as the number of bits per T_N increase. It is evident in Figure 3.12 that the norm of the correlation matrix of COWHC spreading sequences exponentially decreases as the number of bits/T_N increases, while for Hadamard and Gold codes the norm is much higher than COWHC and does not decrease with the increase of bits/T_N. This result indicates that the power of the effect of the residual

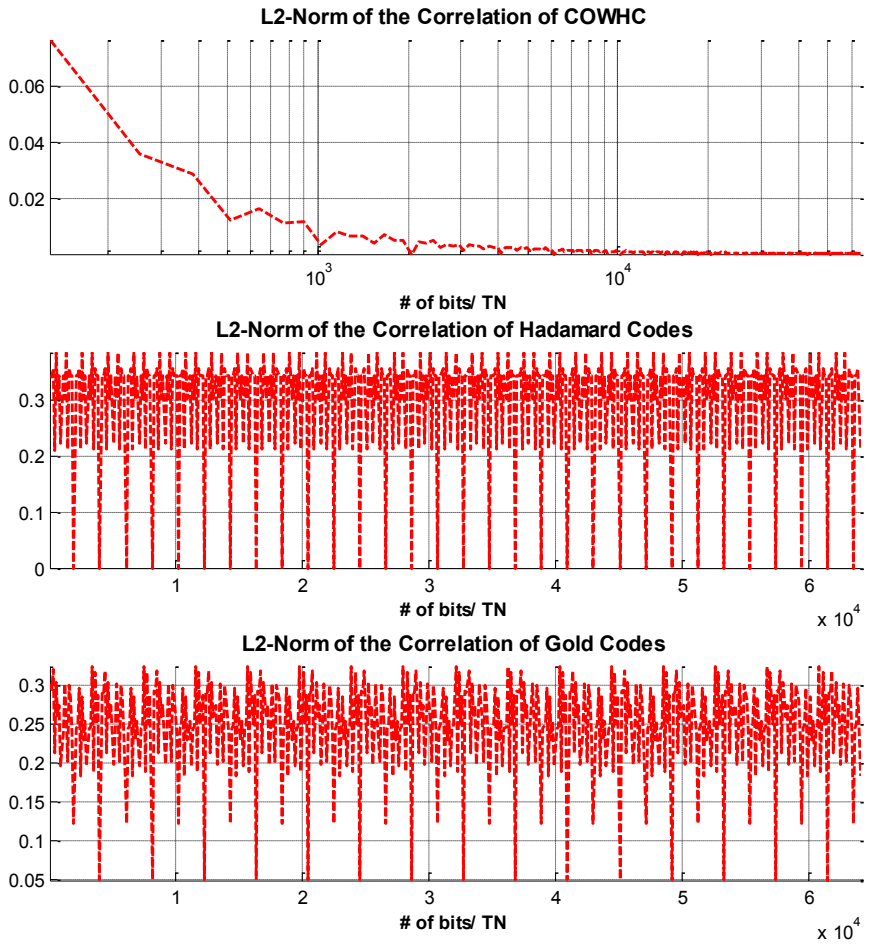

Figure 3.12: The L2-Norm of the correlation of asynchronous COWHC, Hadamard and Gold codes

correlation of COWHC spreading sequences approaches zero as the size of spread signal increases, which approaches the theoretical results when the codes are cyclic rather than shifted in time.

3.6 Conclusions

This chapter introduced the theoretical and implementation details of Cyclic Orthogonal Walsh Hadamard Codes, a special set of spreading codes that are cyclically orthogonal

in all time shits. This special property can contribute to the mitigation of MAI in asynchronous CDMA-based WBANs. The presented codes are simulated and compared to existing spreading codes commonly used in this application. The results shown herein confirm that the performance of the codes when examined from the link BER point of view outperform conventional spreading codes such as Hadamard, Gold and chaotic codes in suppressing the effect of multiple access interference.

Chapter 4

Proposed CDMA-based Wireless Body Area Network

This chapter investigates the second proposed contribution of this thesis document, the CDMA-based WBAN. First, the communication system where information about data gathering, spreading mechanism, channel model and receiving mechanism is introduced. Then simulation results are presented that examine the BER performance of multiple system configurations in order to find the ideal design for the medical WBAN application. Finally, a summary of the contributions and findings presented in this chapter is provided.

4.1 WBAN System Model

This section investigates a proposed CDMA-based body centric wireless sensor network consisting of multiple biosensors denoted by $\mathcal{S}_1, \mathcal{S}_2, \cdots, \mathcal{S}_K$ that communicate wirelessly to the CCU as shown in Figure 2.2 where each $\mathcal{S}_i$, $i = 1, ..., K$ transmits its packets in a single-hop to the CCU and all $\mathcal{S}_i$ transmit their data over a common frequency band. There exists a proactive communication between the biosensors and the CCU which means that each $\mathcal{S}_i$ transmits the same amount of data per time unit to the CCU in a periodic fashion. The data transmitted by $\mathcal{S}_i$ is statistically independent of the data

transmitted by $\mathcal{S}_j$, $i \neq j$. Given the nature of network design in WBANs as described in Section 2.2.2, sensor nodes have power-constrained batteries contrary to the CCU which can have a power source. Hence there is a need to reduce the overall power consumption and computational complexity of the sensor nodes to prolong the lifetime of the network. For this purpose, the proposed WBAN utilizes the duty-cycling mechanism presented in Section 2.2.1 which achieves a significant energy saving in both circuit and signal transmission [4].

4.1.1 Data Gathering Mechanism

To make the network inherently tolerant to failure of individual sensors, it is assumed that the biosensors are unaware of the other nodes' wake up processes. The measured raw signal from sensors $\mathcal{S}_1, \mathcal{S}_2, \cdots, \mathcal{S}_K$ are initially passed through the amplification and filtering processes to increase the signal strength and remove unwanted signals and noise. After digitizing the analog signal using an ADC, an L_i -bit message sequence $X_i \triangleq \{m_\ell\}_{\ell=1}^{L_i}$ is generated, where $m_\ell \in \{-1, +1\}$ and L_i is assumed to be fixed for the node $\mathcal{S}_i$ and is not necessarily the same as L_j for the node $\mathcal{S}_j$, $j \neq i$. Without loss of generality and for ease of analysis, the bit duration of m_ℓ, denoted by T_b is assumed to be the same for all nodes.

4.1.2 Modulation and Spreading Mechanism

In the proposed CDMA-based transmitter, the bit stream X_i is first modulated by a predetermined modulation scheme and then spread as shown in Figure 4.1.

Digital Modulation: involves two subprocess, (a) bit to symbol conversion, and (b) symbol mapping. Bit to symbol conversion translates every l bits from the input message signal to one of $M = 2^l$ symbols, while symbol mapping involves "mapping" the M symbols into the In-phase (I) and Quadrature (Q) plane as shown in Fig. 4.2. Modulation is implemented in digital communication systems to efficiently use bandwidth and

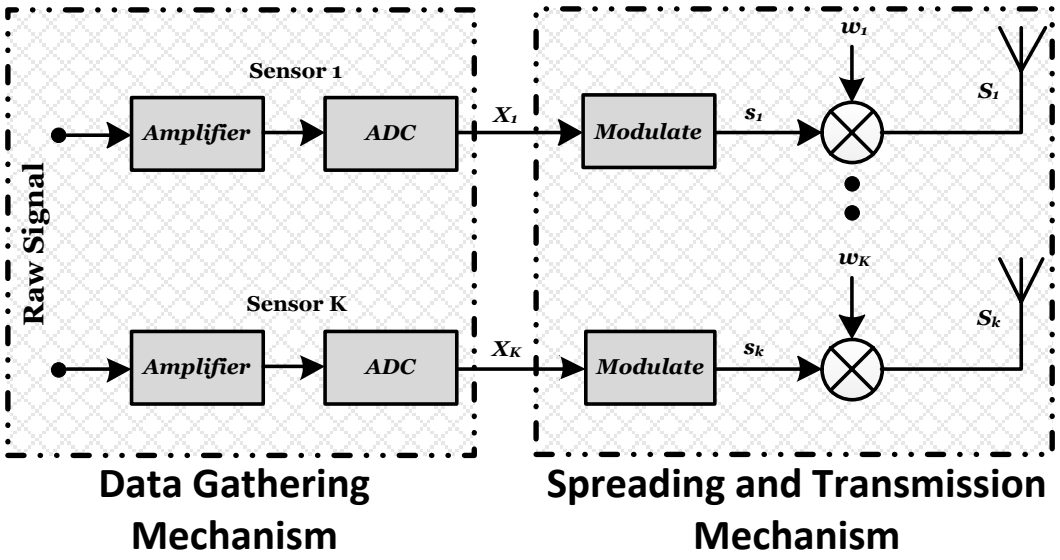

Figure 4.1: Model diagram of the CDMA-based WBAN transmitter

limited frequency resources. There exists a number of modulation schemes used in digital communication systems, ranging from Amplitude Shift Keying (ASK), Frequency Shift Keying (FSK) and Phase Shift Keying (PSK). In ASK the presented bits are represented by different signal amplitudes, while in FSK the frequency is varied for different symbols, and in PSK the phase of the transmitted signal is varied for different symbols.

In CDMA-based WBANs that typically utilize the narrowband physical layer design of the IEEE 802.15.4 [19] and IEEE 802.15.6 [30] standards, only a handful of modulation

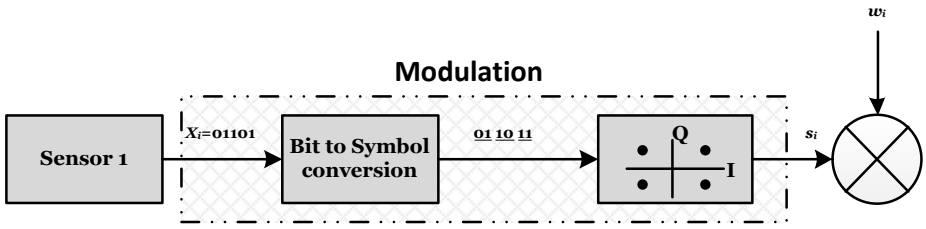

Figure 4.2: Block diagram depicting the digital modulation process at the transmitter

techniques are used. For the proposed WBANs, implemented are the following set of typical modulation techniques [34, 46, 47, 48, 49, 19, 30]:

1. ***Binary Phase Shift Keying (BPSK)***
2. ***Quadrature Phase Shift Keying (QPSK)***
3. ***Offset - Quadrature Phase Shift Keying (OQPSK)***
4. $\pi/2$ ***- Differential Binary Phase Shift Keying (***$\pi/2$***-DBPSK)***
5. $\pi/4$ ***- Differential Quadrature Phase Shift Keying (***$\pi/4$***-DQPSK)***

Detailed technical information pertaining the above modulation schemes are found in Appendix B.

Data Spreading: the modulated signal is directly multiplied by a pseudorandom spreading sequence w_i with chip duration T_c and processing gain N. It is assumed that N is fixed for all $\mathcal{S}_i$ nodes (Section 2.2.1). Denoting s_i as the modulated signal from sensor $\mathcal{S}_i$, $i = 1, ..., K$ as shown in Figure 4.1, the received signal at the CCU contains the spread signal from all sensors $\mathcal{S}_1, \mathcal{S}_2, \cdots, \mathcal{S}_K$ and is given by:

$$\mathcal{X}_r = \sum_{i=1}^{K} w_i s_i + \eta, \tag{4.1}$$

where w_i are unique pseudorandom spreading codes, and η is AWGN.

4.1.3 Channel Model

The specific topology of the proposed network and the choice of low transmission power result in several consequences in the channel model design. It is shown in [50] that a low transmission power implies a small range. The distance between each $\mathcal{S}_i$ and the CCU is short (no longer than 10 m). For this short-range transmission scenario, the channel is multi-path in nature and behaves like a WLAN in a typical indoor office setting. On

the other hand, it is shown in [51] and [52] that the Root Mean Square (RMS) delay spread for indoor applications is in the order of nanoseconds which is small compared to the symbol duration $T_s = 1.66\mu s$ to $T_s = 5.33\mu s$ obtained from the Narrowband PHY Specifications of the IEEE 802.15.6 standard draft [30, 53]. Thus, it is reasonable to expect a flat-fading channel model for the proposed on-body WBAN. In addition, the channel is almost stationary due to the very slow movement of patients compared to the duration of communications. Furthermore, many transmission environments regarding to the on-body WBANs include significant obstacle and structural interference by obstacles (such as wall, doors, and furniture), which leads to reduced Line-Of-Sight (LOS) components. This behaviour suggests a Rayleigh fading channel model. Under the above considerations, the channel model between each biosensor and the CCU is assumed to be a memoryless Rayleigh flat-fading with path-loss. This assumption is used in many works in the literature (i.e. see [36] for CDMA-based WBANs). The fading channel coefficient corresponding to symbol ℓ of node $\mathcal{S}_i$ is denoted as $h_{i,\ell}$, where the amplitude $\left|h_{i,\ell}\right|$ is Rayleigh distributed with Probability Density Function (PDF) $f_{|h_{i,\ell}|}(r) = \frac{2r}{\Omega} e^{-\frac{r^2}{\Omega}},\ r \geq 0$, where $\Omega \triangleq \mathbb{E}\left[|h_{i,\ell}|^2\right]$ [38].

For a ξ^{th}-power path-loss channel of the link between an arbitrary $\mathcal{S}_i$ and the CCU separated by distance d_i, the channel gain factor is given by $\mathcal{L}_{d_i} = M_l d_i^{\xi} \mathcal{L}_1$, $i \in \mathcal{K}$, where M_l is the gain margin which accounts for the effects of hardware process variations, background noise and $\mathcal{L}_1 \triangleq \frac{(4\pi)^2}{\mathcal{G}_t \mathcal{G}_r \lambda^2}$ is the gain factor at $d = 1$ meter which is specified by the transmitter and receiver antenna gains $\mathcal{G}_t$ and $\mathcal{G}_r$, and wavelength λ (e.g. [54]). As a result, when both fading and path-loss are considered, the instantaneous channel coefficient between $\mathcal{S}_i$ and the CCU nodes corresponding to symbol ℓ becomes $G_{i,\ell} \triangleq \frac{h_{i,\ell}}{\sqrt{\mathcal{L}_{d_i}}}$.

4.1.4 Receiver Design and Decoding Mechanism

At the CCU the purpose is to reliably decode for the transmitted signals with minimum interference posed on the desired signals. The receiver antenna captures the transmitted signal $\mathcal{X}_r$ (refer to (4.1)) which contains the signals from all biosensors that has been passed through the AWGN Rayleigh flat-fading channel. As described in Section 2.5.2, in the proposed CDMA-based WBAN, SUD and MUD receiving mechanisms are utilized. In single user detection, the CCU design is visualized in Figure 4.3. In order to decode for sensor $\mathcal{S}_i$ the model simply de-spreads $\mathcal{X}_r$ with code w_i as follows:

$$\hat{s}_i = w_i \mathcal{X}_r = \underbrace{{w_i}^2 s_i}_{Desired\ Signal} + \underbrace{\sum_{\substack{j=1 \\ j \neq i}}^{K} w_i w_j s_j}_{Multiple\ Access\ Interference} + \underbrace{w_i \eta}_{Noise} \tag{4.2}$$

It is assumed that the same pre-determined modulation scheme used at the sensor node is used at the CCU, and that w_i for all $\mathcal{S}_i$ is known at the CCU. In (4.2), ${w_i}^2 s_i$ is the desired signal, $\sum_{\substack{j=1 \\ j \neq i}}^{K} w_i w_j s_j$ is the interference of multiple sensors on the desired signal, and $w_i \eta$ is the AWGN. In an ideal synchronous CDMA system where bit-level synchronization can be achieved throughout the system, and if orthogonal spreading codes w_i are used, then by definition in (4.2) ${w_i}^2$ will equal to 1, and $w_i w_j$ will evaluate to zero (due to orthogonality), effectively eliminating the interference. Orthogonal spreading codes will lose their orthogonality due to the asynchronous nature of WBANs (Figure 3.6). Hence in the proposed CDMA-based WBAN, the system performance will be compared with a variety of spreading codes including the proposed COWHC (Section 3.2), conventional Hadamard codes (Section 3.1), Gold and Chaotic codes (Section 2.5.1).

Further to the SUD receiver design, the proposed CDMA-based WBAN implements a MUD decorrelating receiver (Section 2.5.2) which will be used to compare performance results of non-cyclic orthogonal spreading codes to that of COWHC, as the decorrelating receiver is designed to compensate for the cross-correlation of spreading codes.

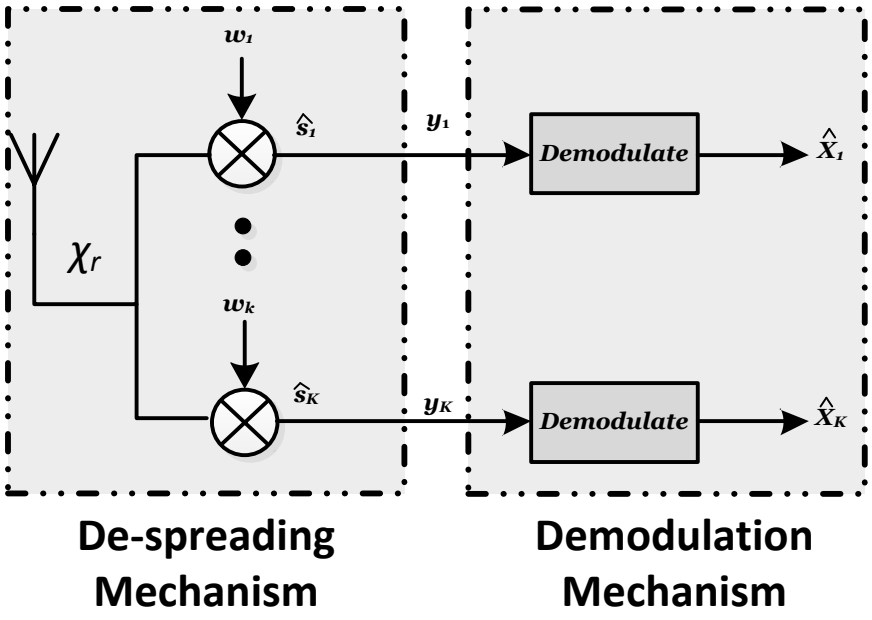

Figure 4.3: Single User Detection (SUD) model at the CCU of CDMA-based WBANs

4.2 Simulation Results

This section studies the performance results of the proposed CDMA-based WBAN model presented in this chapter. The aim is to identify the optimum spreading code, modulation scheme, and receiver design that combined produce the optimum communication model for reliable transmission in body-centric WBANs. The performance will be studied from the link BER point of view (Section 3.3.1) and under minimalistic (Section 3.3.2.1) and ideal (Section 3.3.2.2) network designs.

4.2.1 Conventional Receiver Vs. Decorrelating Receiver

In Chapter 3 the COWHC spreading sequences were simulated in a CDMA-based WBAN that utilizes a conventional SUD receiver as described in Section 4.1.4. Of interest is to compare the performance of the conventional receiver to that of the decorrelating receiver

described in Section 2.5.2. It is worth noting that in theory if the decorrelating receiver is used with COWHC spreading sequences then the correlation matrix **R** in (2.3) would equate to the identity matrix **I** due to the cyclic orthogonal nature of COWHC. But given the effect of asynchronicity in a practical setup where the codes are shifted in time rather than cyclicly shifted, the **R** matrix of COWHC would still have some residual. Through simulation it was found that COWHC in a simple network scenario performs better with a conventional receiver, while for the ideal scenario a decorrelating receiver achieved better BER performance. This is attributed to the fact that when more users exists in the network, the effect of the residual correlation is higher, and the decorrelating receiver can compensate for it much better than the conventional receiver. The parameters for the following simulations are shown in Table 4.1.

Table 4.1: Simulation parameters used for simulating the proposed WBAN

Parameter	Range/ Type	Description
Num_Users	2 and 6	For simple and ideal network designs
N	64	Shown to produce better results in Section 3.5.1
SNR	-10dB to 20dB	Practical channel noise operational range in WBANs
dataLen	1000	1kb/T_N
ittTimes	3000	Iterate over 3000 duty-cycles for accurate estimation
CodeType	'cyclicwalsh', 'noncyclicwalsh', 'gold', and 'chaotic'	Examine the behaviour of proposed and conventional spreading codes
RecType	'conventional' and 'decorrelating'	Compare conventional (SUD) to decorrelating (MUD) receivers
Fading	'yes'	Simulate a Rayleigh flat-fading channel
ModType	BPSK	Simple and highly efficient modulation scheme

BER Performance: in Figure 4.4 the SNR vs BER performance is visualized for the four spreading codes in a simple network model with two users where a conventional receiver was used for COWHC and decorrelating receiver for Hadamard, Gold and chaotic codes, while in Figure 4.5 an ideal network design with 6 users is simulated with

decorrelating receiver utilized for all codes.

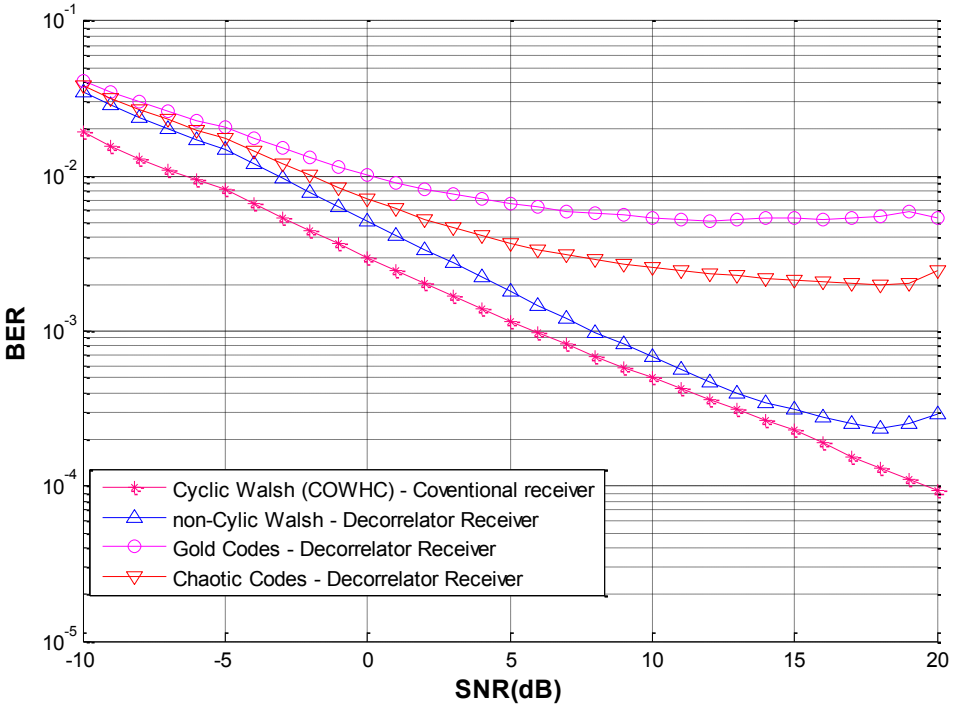

Figure 4.4: SNR vs BER performance results comparing spreading codes in SUD and MUD receivers in a simple 2-user WBAN (N=64)

Performance analysis: in the simple network scenario, when comparing the effect of the decorrelating receiver shown in Figure 4.4 to that of the SUD receiver in Figure 3.8, one can note that: *i*) non-cyclic Hadamard codes produced a much better BER performance when the decorrelating receiver is utilized, *ii*) Gold codes on the other hand performed better with the SUD receiver, and *iii*) chaotic codes maintained the same error floor for both receivers. On the other hand, in the ideal network scenario with 6-users in the network as shown in Figure 4.5, there is no tangible performance gain when compared to that of the conventional receiver visualized in Figure 3.10. This result can be attributed to the effectiveness of the decorrelating receiver at suppressing the

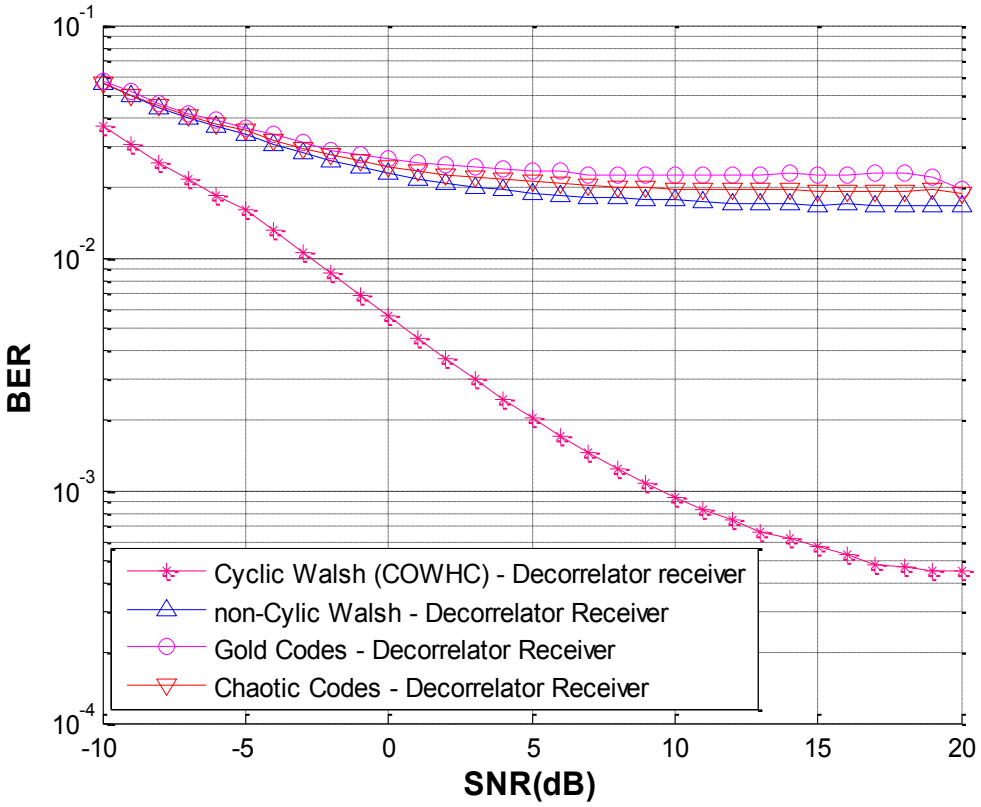

Figure 4.5: SNR vs BER performance results comparing spreading codes in MUD receivers in an ideal 6-user WBAN (N=64)

MAI when high correlation exists amongst the spreading codes. Also, as noted in (2.4) the decorrelating receiver enhances the noise by $\mathbf{R}^{-1}$ which can effectively increase the number of bits decoded in error.

While the decorrelating receiver produces mixed results for conventional spreading codes, it is noted that in both the simple network (Figure 4.4) and ideal network (Figure 4.5), COWHC spreading sequences outperforms Hadamard, Gold and chaotic codes with and without MUD. To combat the drop in performance that was visualized in Section 3.5.2, the performance of the decorrelating receiver for COWHC in an ideal network is shown to effectively compensate for the small correlation residual. While in theory

it is still expected that the ideal 6-user network with COWHC spreading sequences to perform similarly to that of the 2-user scenario, due to the numerical errors the residual correlation contributes to the decoding process as well as the noise enhancement (in the decorrelating receiver), the ideal scenario produces slightly lower BER performance that that of the simple scenario (compare Figure 4.5 to Figure 4.4). The results presented here still affirm that if COWHC are utilized in a CDMA-based WBAN, both a low-complexity single user detection receiver or a decorrelating MUD receiver can be employed to produce BER performance that is marginally lower than conventional spreading codes.

4.2.2 Comparison of Modulation Schemes

Table 4.2: List of the optimum spreading code and receiver design combinations for multiple modulation techniques

	2-user Network	**6-user Network**
BPSK	COWHC - SUD	COWHC - SUD
QPSK	non-cyclic Hadamard - SUD	COWHC - SUD
OQPSK	COWHC - SUD	COWHC - SUD
$\pi/2$-*DBPSK*	COWHC - SUD	COWHC - SUD
$\pi/4$-*DQPSK*	COWHC - SUD	COWHC - SUD

In this simulation the aim is to examine the performance of the proposed CDMA-based WBAN with multiple modulation techniques commonly used in WBANs (Section 4.1.2), namely; BPSK, QPSK, OQPSK, $\pi/2$-DBPSK, and $\pi/4$-DQPSK. A large set of BER simulations were conducted in order to identify the spreading codes that produced optimum BER performance for each of the modulation techniques. For these simulations, a conventional SUD receiver was utilized to study the effect of modulation schemes in a low complexity system design. Table 4.2 summarizes the findings for both a 2-user and 6-user networks with N=64.

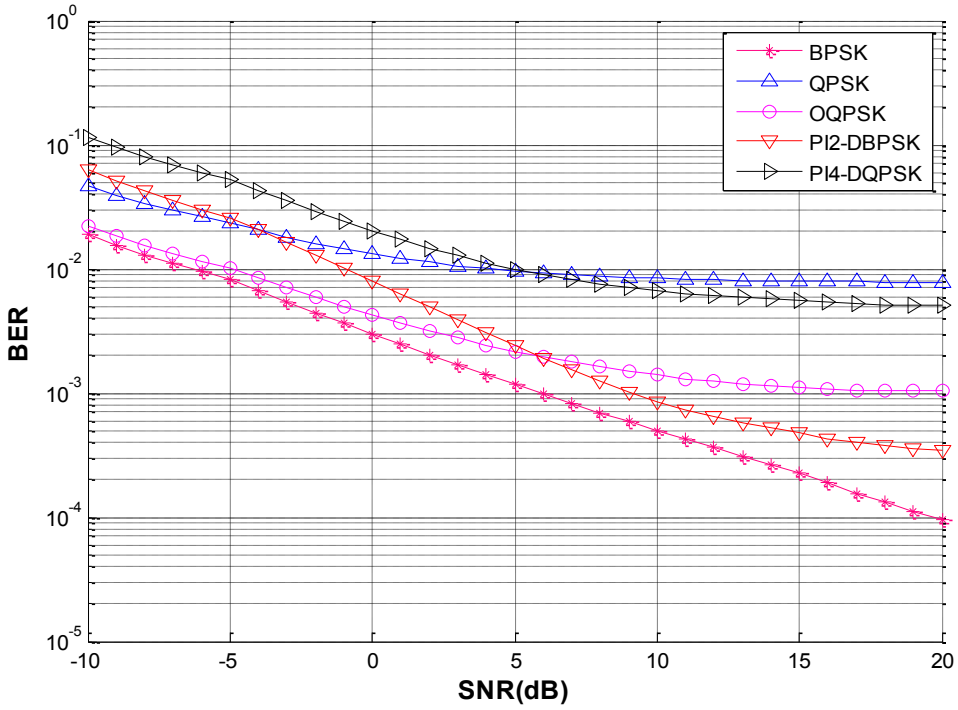

Figure 4.6: SNR vs BER performance results comparing multiple modulation techniques in a simple 2-user WBAN (N=64)

It is evident from Table 4.2 that COWHC produces the optimum performance for the CDMA-based WBAN for most modulation techniques. The one exception was QPSK in a 2-user network setup, where the non-cyclic Hadamard codes utilized with a conventional SUD receiver produced slightly better BER performance than its COWHC counterpart. This however was not the case in the ideal network scenario, where high interference ensured that COWHC with a conventional SUD receiver was the optimum combination for QPSK and all other modulation techniques. The BER performance of the combinations shown in Table 4.2 are presented in Figure 4.6 and Figure 4.7.

Performance analysis: the results presented in Figure 4.6 and Figure 4.7 confirms that BPSK is the most robust modulation technique and produces the most optimum

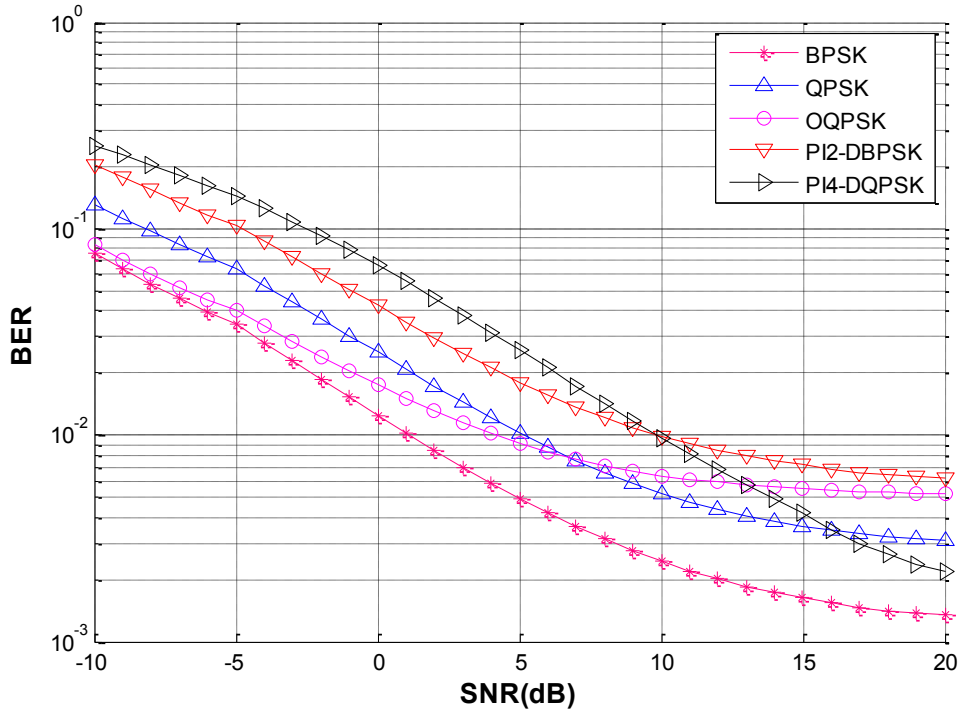

Figure 4.7: SNR vs BER performance results comparing multiple modulation techniques in an ideal 6-user WBAN (N=64)

BER results when utilized in the proposed CDMA-based WBAN. It is worth noting that to maintain the same transmission bandwidth, quadrature modulations such as QPSK, OQPSK and $pi/4$-DQPSK transmit at twice the data rate of that in binary modulation such as BPSK and $pi/2$-DBPSK. Hence it is worth studying the performance of quadrature modulations in Figure 4.6 and Figure 4.7. In the simple network scenario OQPSK outperforms both QPSK and $pi/4$-DQPSK across the SNR range, while in the ideal network scenario OQPSK is the better quadrature modulation technique in noisy environments (SNR $<$ 7 dB) and QPSK is superior when SNR $\geq$ 7dB. Hence using QPSK or OQPSK will not produce the optimum BER performance when compared to BPSK, but instead, twice the transmission data rate can be achieved.

4.3 Conclusions

This chapter studied the implementation details of the proposed CDMA-based communication system to be used for wireless medical body area networks. Of interest is studying the effect of multiple modulation techniques and receiver designs on the network performance from the BER point of view. The presented simulation results show that utilizing multiple user detection techniques at the receiver can improve the result of conventional spreading codes such as Hadamard and chaotic codes, though it does not outperform COWHC spreading codes with a conventional SUD receiver. This shows that given the application and system design, employing COWHC spreading codes with a low complexity SUD receiver can achieve better BER performance than conventional spreading codes. It was also shown that utilizing the decorrelating receiver for COWHC can significantly reduce the residual correlation generated from the shift in time amongst the sensors. This chapter also presented simulation results that studied the effect of modulation on the overall BER performance, and it was shown that BPSK can achieve better BER across the spectrum. On the other hand QPSK and OQPSK were outperformed by BPSK, but they showed tangible performance that can be used in networks that would require support for higher data rates. Overall, a design that encompasses COWHC, BPSK modulation and a conventional receiver was the optimum design choice that produced the lowest BER compared to conventional solutions. On the other hand, utilizing a slightly more complex decorrelating receiver can further enhance the BER performance of COWHC in CDMA-based WBANs.

Chapter 5

Conclusions

5.1 Research Discussion and Summary

This thesis presented two contributions that are designed for medical based wireless body area networks where multiple biosensors communicate simultaneously and over the same frequency band to a central node. The asynchronous nature of WBANs and the non-orthogonality of spreading codes produce multiple access interference at the central node, which contributes to decoding errors and lowers link reliability. The first contribution discussed a special set of Hadamard codes namely COWHC that maintain their orthogonality in the asynchronous operation of WBANs. The cyclic orthogonality property of COWHC was studied and a methodology for code selection was demonstrated. Then by using the BER as a validation metric, the performance of COWHC spreading sequences was examined in a simulated CDMA-based WBAN. The COWHC BER results when compared to conventional spreading codes such as Gold and chaotic codes, produced a marginally lower BER across a practical SNR range, while conventional codes had an error floor at SNR values above 10dB. The utilization of COWHC spreading sequences in CDMA-based WBANs is shown to effectively mitigate MAI at the CCU. The one shortcoming of COWHC is that the number of cyclic orthogonal codes produced from

the 2^k square Hadamard matrix is limited to $K = k+1$, which limits the total number of sensors in the WBAN to K. But since biosensors intervene with the comfort of the user (patient), the design of such networks must consider low device count in the first place [16]. Hence in a typical network with 6 sensors, COWHC can be generated from the $\mathbf{H}_{32}$ Hadamard matrix, which ensures a spreading factor of N=32. On the contrary, if more sensor nodes are required, a higher spreading factor must be utilized which inherently increases the signal bandwidth (i.e. N=512 for 10 sensors).

The second contribution of this thesis presented a study of a CDMA-based WBAN from the modulation and receiver design point of view. It was found through simulations that a MUD receiver such as the decorrelating receiver can lower the effect of non-orthogonality for conventional spreading codes such as Hadamard codes and chaotic codes. Though even with the added complexity of the decorrelating receiver, the utilization of conventional codes did not mitigate the effect of MAI as efficiently as COWHC in the asynchronous WBAN. When used for spreading, COWHC performed better from a BER point of view with a conventional SUD receiver than Hadamard or chaotic codes with a MUD receiver. This ensured that when used in CDMA-based WBANs, COWHC can effectively reduce the complexity of receiver design by only requiring conventional single user detection to achieve accurate decoding performance. On the contrary, if a decorrelating receiver is utilized with COWHC, further performance gain is visualized from the BER. In addition to receiver design, the proposed CDMA-based WBAN studied the effect of multiple PSK modulation schemes on the communication link. It was shown that BPSK modulation was the most robust at accounting for noise in the channel and outperformed other PSK modulations throughout the SNR range. It is worth mentioning that while quadrature modulation such as QPSK and OQPSK were not optimum when compared to BPSK, they support double the data rate of that in BPSK. This is because quadrature PSK encode two bits per symbol of the raw message signal and the transmitted signal bandwidth is maintained the same for both binary and quadrature

modulations. Hence QPSK and OQPSK might be of preference for applications with higher data rate.

Through the design and simulation of COWHC and CDMA-based WBAN, this thesis identifies that a CDMA WBAN with COWHC spreading codes, BPSK modulation and a conventional SUD receiver produce marginally better BER performance than conventional spreading codes, modulations schemes and receivers commonly used in this application. Furthermore, utilizing a slightly more complex decorrelating receiver at the CCU can further enhance the BER performance of COWHC in CDMA-based WBANs.

5.2 Future Work

Due to the span of the presented work into a number of areas pertaining to the design of the communication system, a number of design and parameter assumptions were used to narrow the scope of the study. Future work in this area can examine the following:

- The performance of the proposed work was only studied from the BER point of view. While this validation metric is sufficient to study the impact of the proposed contributions on the packet collision and MAI in WBANs, it is of prime importance to study the effect of COWHC, receiver design and modulation on the performance of WBANs from the energy consumption and network throughput points of view.

- While MUD receivers might not be suitable for the aforementioned WBAN due to low sensor numbers in the network, they are well suited in fully loaded networks where $K = 2^k$ (contrary to $K \leq k + 1$). The effects of MUD receivers in larger WBANs should be studied in the future. Also, ways to better utilize COWHC in WBANs with more sensors in the network than the typical should be studied.

- The channel was assumed to be a memoryless Rayleigh flat-fading channel. The effect of the failure of this assumption on the system should be studied in the future.

- It was assumed that the CCU has full knowledge of the channel state, which in practice is not true. The effect of channel estimation at the CCU should be studied in future work.

Appendix A

History of Wireless Standards for WBANs

A.1 Wireless Medical Telemetry Services (WMTS)

In order to provide wireless medical telemetry with licensed spectrum the FCC in the United States introduced Wireless Medical Telemetry Services (WMTS). This standard was licensed by rule and no individual licenses are required. In the early 2000s hospitals that were using the unlicensed TV channel bands for their telemetry had upgraded their equipment to support WMTS. WMTS included three unique bands for transmission; 608-614 MHz, 1395-1400 MHz, and 1427-1432 MHz [55]. While WMTS provided special bands for medical telemetry, these bands were still embedded within the HDTV bands and interfering signals from near by channel bands remained an issue [28]. WMTS posed a number of limitations such as: no international recognition, restricted bandwidth and lack of protection against existing channel interference which prevented it from being the favourite wireless standard for WBANs.

A.2 Wireless Local Area Network (WLAN)

The introduction of IEEE 802.11 standards such as 802.11, 802.11a and 802.11c was done before WMTS. The purpose of these standards is the implementation of Wireless Local Area Networks (WLANs), which are networks that cover a small geographical location. Collectively these 802.11 standards are known as Wi-Fi. They operate over the following bands: 2.4GHz and 5GHz. Ever since the adaptation of 802.11 there has been many variations such as 802.11g that were introduced to effectively boost the supported bandwidth as well as the range and 802.11n which introduced MIMO (Multiple Input Multiple Output) technologies to existing 802.11g devices. WLAN has been used for WBANs in numerous occasions [28, 56].

A.3 Medical Implants Communication Services (MICS)

Medical Implants Communication Services (MICS) is a standard developed specifically for ultra-low power, unlicensed medical implant devices. The standard introduced by the FCC in the United States operates in the 402-405 MHz band and can support data rates of up 16 kbps with a range of 0-2m. The standard allows bidirectional communication between the implant device and the CCU with a maximum bandwidth of 300 KHz. The selection of the 402-405 MHz band was chosen such that it satisfies the MICS requirements with respect to the size of device, power, antenna performance and receiver design, and is compatible with international frequency allocations [57]. MICS can be used for implant devices available within a bigger WBAN system.

A.4 IEEE 802.15.4 - ZigBee

IEEE 802.15.4 defines a set of specifications for Low-Rate Wireless Personal Area Networks (LR-WPANs). WPANs are networks that operate in the vicinity of the human body, with a range of approximately 10 meters [19], and devices that consume minimal power. ZigBee utilizes two frequency bands, 868/ 915 MHz and 2.4 GHz with data rates of 40 and 250 kbps, respectively. ZigBee also utilizes two network topologies, Star Network, and Peer-to-Peer, with two different types of devices, Full-Function Device (FFD) and Reduced-Function Device (RFD). A FFD can operate as a coordinator and a device (such as the CCU) and can communicate with RFDs and other FFDs, while RFDs make up the sensor nodes. Binary Phase Shift Keying (BPSK) and Offset-Quadrature Phase Shift Keying (OQPSK) are the two suggested modulation schemes in ZigBee. It also utilizes Direct Sequence Spread Spectrum (DSSS) for spreading.

ZigBee has been the ideal protocol for use in WBANs since its introduction and has been ideal for networks with low data rate and low power devices. Many see ZigBee to be limited as it only supports devices with low data rates. Since, there has been a number of proposals such as 802.15.4a [58] which uses the Ultra Wide Band (UWB) 3.1-10.6 GHz band to support higher data rates, but the standard still posses high loss and cannot be used for medical implants.

Appendix B

Digital Modulation

B.1 Binary Phase Shift Keying (BPSK)

Binary Phase Shift Keying is the simplest form of PSK in which bits 0 and 1 are represented by two points on the I-Q plane with an π phase separation. The most general constellation form of BPSK is shown in Figure B.1. While BPSK is the most robust PSK modulation technique, it is impractical for use in high data rate applications due to the fact that it is only capable of modulating at 1 bit/symbol.

Mathematically, BPSK follows the equation:

$$\mathbf{s}_k(t) = \sqrt{\frac{2E_s}{T_s}} \cos\left(2\pi f_c t + \pi(1-k)\right) \quad , \quad k = 0, 1 \tag{B.1}$$

where E_s is the symbol energy (also E_b in BPSK), T_s is symbol period (also T_b in BPSK), and f_c is the center frequency. Equation B.1 produces two phases, 0 and π respectively. Hence the signals are generally presented as $\sqrt{E_b}\theta(t)$ for 1, and $-\sqrt{E_b}\theta(t)$ for 0, where $\theta(t)$ refers to the basis function and is defined as follows:

$$\theta(t) = \sqrt{\frac{2}{T_b}} \cos\left(2.\pi.f_c.t\right) \tag{B.2}$$

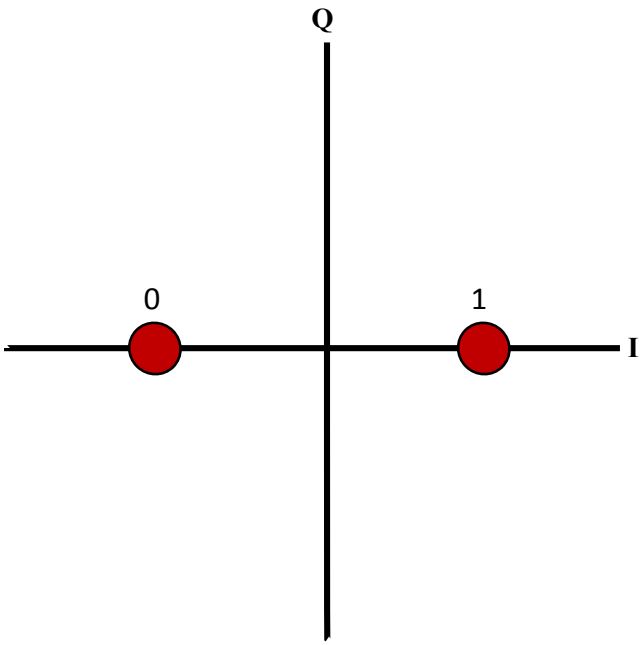

Figure B.1: Constellation diagram for BPSK

B.2 Quadrature Phase Shift Keying (QPSK)

Quadrature Phase Shift Keying uses four points equispaced ($\pi/2$ phase separation) on a circle in the I-Q plane. With the four possible phases, QPSK can modulate at a rate of 2 bits/symbol. A possible constellation is shown in Figure B.2 where gray coding is used. Generally speaking QPSK is used to either double the data-rate and maintain same bandwidth compared to BPSK modulation, or to maintain data-rate and half the bandwidth required for transmission.

Gray coding as used in the constellation diagram refers to the arrangement of symbols such that transition from one symbol to the next involves only one bit change. As shown in Figure B.2, the transitions from symbols 00 to symbol 01, 01 to 11, 11 to 10, and 10 to 00 each requires one of the two bits to change. Gray coding is used in digital communications in order to facilitate error correction and reduce the BER.

Mathematically, QPSK follows the equation:

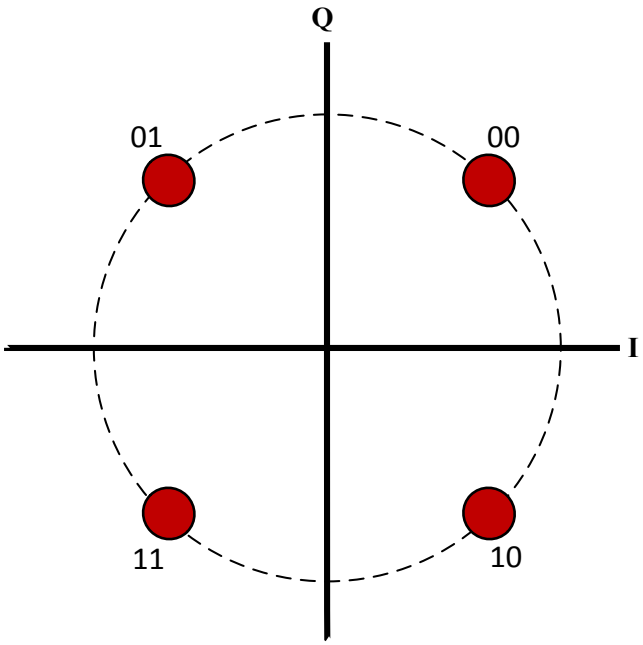

Figure B.2: Constellation diagram for QPSK

$$\mathbf{s}_k(t) = \sqrt{\frac{2E_s}{T_s}} \cos\left(2\pi f_c t + \frac{\pi}{4}(2k-1)\right) \quad , \quad k = 1, 2, 3, 4 \tag{B.3}$$

Equation B.3 produces two phases, $\pi/4$, $3\pi/4$, $5\pi/4$ and $7\pi/4$ respectively. Hence the signal space is a two dimensional one with $\theta_1(t)$ and $\theta_2(t)$ as follows:

$$\begin{aligned} \theta_1(t) &= \sqrt{\tfrac{2}{T_s}} \cos\left(2.\pi.f_c.t\right) \\ \theta_2(t) &= \sqrt{\tfrac{2}{T_s}} \sin\left(2.\pi.f_c.t\right) \end{aligned} \tag{B.4}$$

and hence the constellation points take the values of $(\pm\sqrt{\frac{E_s}{2}}, \pm\sqrt{\frac{E_s}{2}})$ in the signal space.

B.3 Offset Quadrature Phase Shift Keying (OQPSK)

Offset Quadrature Phase Shift Keying is a variant of the QPSK modulation explained in Section B.2. In traditional QPSK taking two bits at a time in order to construct a symbol will allow the phase to shift by up to π from symbol to the next. This π

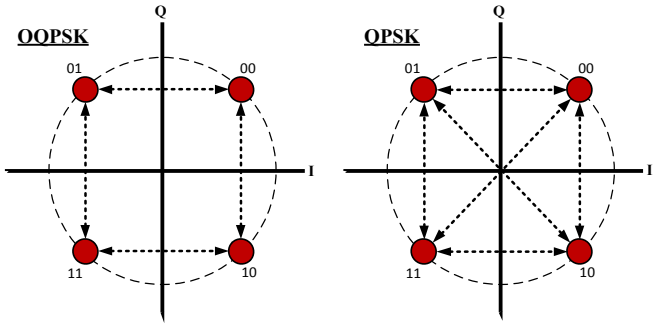

Figure B.3: Constellation diagram for OQPSK

shift causes large fluctuations in amplitude after filtering the signal. In order to combat this problem, OQPSK introduces an offset of $T_s/2$ (equivalently T_b) to the quadrature data stream. This process insures that a maximum phase shift of $\pi/2$ can occur every T_s, hence produce amplitude variations less than QPSK while maintaining the same bandwidth efficiency. In Figure B.3 I show the difference between OQPSK and QPSK in terms of possible phase changes from symbol to the next.

B.4 $\pi/2$- Differential Binary Phase Shift Keying ($\pi/2$-DBPSK)

Differential encoded phase shift keying involves the changing of the carrier phase according to the symbol to be transmitted. In differentially encoded BPSK the phase may change by π radians if '1' is to be transmitted, and 0 radians if '0' is to be transmitted, and so on. This technique removes some of the phase ambiguity that can arise from the effects of the channel.

In $\pi/2$- Differential Binary Phase Shift Keying the constellation diagram is made of two standard BPSK constellations (Fiure B.1) shifted by $\pi/2$. Hence the constellation of $\pi/2$-DBPSK involves four constellation points, and inherently insures that phase transitions are limited to $\pi/2$ between any two symbols as shown in Figure B.4.

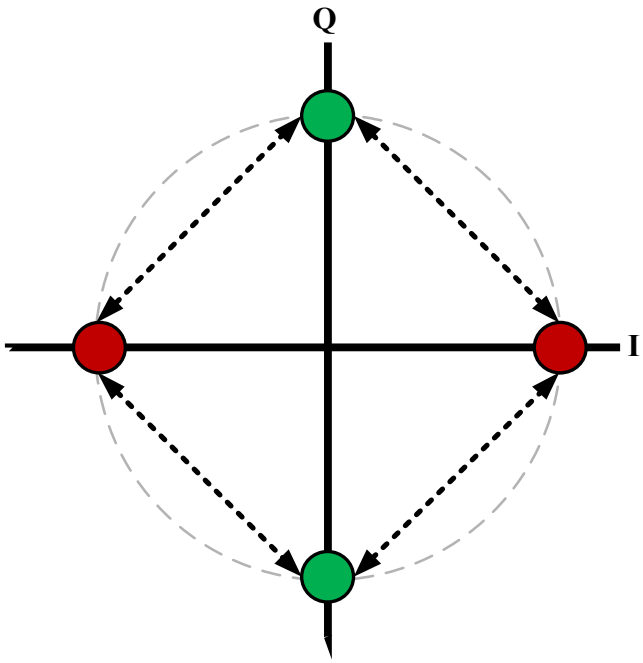

Figure B.4: Constellation diagram for $\pi/2$-DBPSK

B.5 $\pi/4$- Differential Quadrature Phase Shift Keying ($\pi/4$-DQPSK)

$\pi/4$- Differential Quadrature Phase Shift Keying is a modified version of the standard QPSK modulation with phase transitions restricted to $\pm\pi/4$ and $\pm 3\pi/4$. The constellation of the $\pi/4$-DQPSK consists of two standard QPSK constellations (Figure B.2) that are shifted by $\pi/4$, hence totaling eight constellation points as shown in Figure B.5

For example, if a $\pi/4$-DQPSK has $+\pi/4$, $+3\pi/4$, $-3\pi/4$, and $-\pi/4$ as phase shifts that correspond to symbols 00, 01, 11, and 10 respectively, and the current phase is $\pi/2$ radians, then the possible phase shifts for the next symbol are shown in Figure B.6.

In the proposed IEEE 802.15.6 [30], $\pi/8$-D8PSK modulation is an optional choice in the Narrowband physical layer design. $\pi/8$-D8PSK is implemented similarly to $\pi/4$-DQPSK but with 8-PSK as the base modulation scheme.

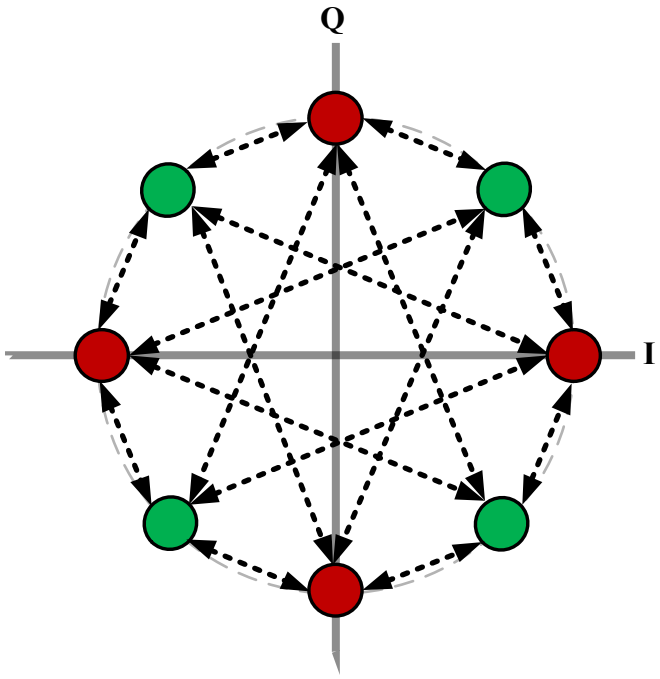

Figure B.5: Constellation diagram for $\pi/4$-DQPSK

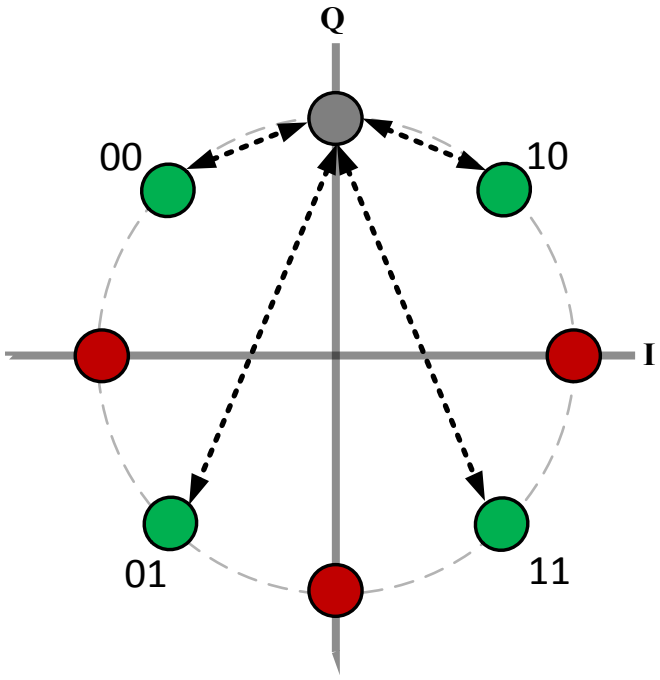

Figure B.6: Sample phase shift for $\pi/4$-DQPSK

Bibliography

[1] Benoît Latré, Bart Braem, Ingrid Moerman, Chris Blondia, and Piet Demeester, "A survey on wireless body area networks," *Wirel. Netw.*, vol. 17, pp. 1–18, January 2011.

[2] Jamil. Y. Khan and Mehmet R. Yuce, *New Developments in Biomedical Engineering*, InTech, 2010.

[3] Mehmet R. Yuce and Chee Keong Ho, "Implementation of body area networks based on mics/wmts medical bands for healthcare systems," in *Engineering in Medicine and Biology Society, 2008. EMBS 2008. 30th Annual International Conference of the IEEE*, aug. 2008, pp. 3417 –3421.

[4] J. Abouei, J.D. Brown, K.N. Plataniotis, and S. Pasupathy, "Energy efficiency and reliability in wireless biomedical implant systems," *Information Technology in Biomedicine, IEEE Transactions on*, vol. 15, no. 3, pp. 456 –466, may 2011.

[5] M. Salehi J. G. Proakis, *Digital Communications*, New York: McGraw-Hill, fifth edition, 2008.

[6] J.M.L.P. Caldeira, J.J.P.C. Rodrigues, and P. Lorenz, "Toward ubiquitous mobility solutions for body sensor networks on healthcare," *Communications Magazine, IEEE*, vol. 50, no. 5, pp. 108 –115, may 2012.

[7] R. Schmidt, T. Norgall, J. Mrsdorf, J. Bernhard, and T. Von Der Grn, "Body area network BAN: a key infrastructure element for patient-centered medical applications," *Biomed Tech (Berl)*, vol. 47, pp. 365–368, Jan. 2002.

[8] J.A. Warren, R.D. Dreher, R.V. Jaworski, J.J. Putzke, and R.J. Russie, "Implantable cardioverter defibrillators," *Proceedings of the IEEE*, vol. 84, no. 3, pp. 468 –479, mar 1996.

[9] Sana Ullah, Pervez Khan, Niamat Ullah, Shahnaz Saleem, Henry Higgins, and Kyung Sup Kwak, "A review of wireless body area networks for medical applications," *CoRR*, vol. abs/1001.0831, 2010.

[10] Federal Communications Commission (FCC), "Federal communications commission (fcc) - spectrum bands," 2012.

[11] Industry Canada, "Radio spectrum allocations in canada," 2007.

[12] Wen-Bin Yang and K. Sayrafian-Pour, "A ds-cdma interference cancellation technique for body area networks," in *Personal Indoor and Mobile Radio Communications (PIMRC), 2010 IEEE 21st International Symposium on*, Sept. 2010, pp. 752 –756.

[13] R. Gold, "Optimal binary sequences for spread spectrum multiplexing," *IEEE Trans. on Inform. Theory*, vol. 8, pp. 619–621, Oct. 1967.

[14] I. Martoyo, Philip, A. Susanto, E. Wijanto, H. Kanalebe, and K. Gandi, "Chaos codes vs. orthogonal codes for cdma," in *Spread Spectrum Techniques and Applications (ISITA), 2010 IEEE 11th International Symposium on*, oct. 2010, pp. 189 –193.

[15] K. Benkic, "Proposed use of a cdma technique in wireless sensor networks," in *Systems, Signals and Image Processing, 2007 and 6th EURASIP Conference focused*

on Speech and Image Processing, Multimedia Communications and Services. 14th International Workshop on, June 2007, pp. 343 –348.

[16] Sana Ullah, Henry Higgins, Bart Braem, Benoit Latre, Chris Blondia, Ingrid Moerman, Shahnaz Saleem, Ziaur Rahman, and Kyung Kwak, "A comprehensive survey of wireless body area networks," *Journal of Medical Systems*, pp. 1–30, 10.1007/s10916-010-9571-3.

[17] A. Y. Wang, S.-H. Cho, C. G. Sodini, and A. P. Chandrakasan, "Energy efficient modulation and MAC for asymmetric RF microsensor systems," in *Proc. of International Symposium on Low Power Electronics and Design (ISLPED'01)*. Huntington Beach, Calif, USA, Aug. 2001, pp. 106–111.

[18] I.F. Akyildiz, Weilian Su, Y. Sankarasubramaniam, and E. Cayirci, "A survey on sensor networks," *Communications Magazine, IEEE*, vol. 40, no. 8, pp. 102 – 114, aug 2002.

[19] IEEE Standards, "Part 15.4: Wireless Medium Access control (MAC) and Physical Layer (PHY) Specifications for Low-Rate Wireless Personal Area Networks (WPANs)," *IEEE 802.15.4 Standards*, Sept. 2006.

[20] Changle Li, Huan-Bang Li, and R. Kohno, "Performance evaluation of ieee 802.15.4 for wireless body area network (wban)," in *Communications Workshops, 2009. ICC Workshops 2009. IEEE International Conference on*, june 2009, pp. 1 –5.

[21] J. Zeng, H. Minn, and L. S. Tamil, "Time hopping direct-sequence CDMA for asynchronous transmitter-only sensors," in *Proc. IEEE Military Communications Conference (MILCOM'08)*, Nov. 2008.

[22] Yung-Cheng Wu, Tzu-Yun Lai, Tzu-Shiang Lin, Jiing-Yi Wang, Jyh-Cherng Shieh, Joe-Air Jiang, Wen-Dien Chang, Chien-Tsung Tsai, and Chien-Kang Hsu, "A wsn-

based wireless monitoring system for intradialytic hypotension of dialysis patients," in *Sensors, 2009 IEEE*, oct. 2009, pp. 1959 –1962.

[23] J. P. Kooman F. M. Sande and K. M. L. Leunissen, "Intradialytic hypotension - new concepts on an old problem," in *Nephrol Dial Transplant*, 2000, vol. 15, pp. 1746–1748.

[24] K.J. Kappiarukudil and M.V. Ramesh, "Real-time monitoring and detection of "heart attack" using wireless sensor networks," in *Sensor Technologies and Applications (SENSORCOMM), 2010 Fourth International Conference on*, july 2010, pp. 632 –636.

[25] F. Sufi, Qiang Fang, I. Khalil, and S.S. Mahmoud, "Novel methods of faster cardiovascular diagnosis in wireless telecardiology," *Selected Areas in Communications, IEEE Journal on*, vol. 27, no. 4, pp. 537 –552, may 2009.

[26] E. Dolatabadi and S. Primak, "Ubiquitous wban-based electrocardiogram monitoring system," in *e-Health Networking Applications and Services (Healthcom), 2011 13th IEEE International Conference on*, june 2011, pp. 110 –113.

[27] Wang Weiya, Lu Zhanfeng, Gao Li, and Hu Gui, "Research on wearable ecg monitoring system based on zigbee," in *Cross Strait Quad-Regional Radio Science and Wireless Technology Conference (CSQRWC), 2011*, july 2011, vol. 2, pp. 929 –932.

[28] S.D. Baker and D.H. Hoglund, "Medical-grade, mission-critical wireless networks [designing an enterprise mobility solution in the healthcare environment]," *Engineering in Medicine and Biology Magazine, IEEE*, vol. 27, no. 2, pp. 86 –95, march-april 2008.

[29] K.S. Kwak, S. Ullah, and N. Ullah, "An overview of ieee 802.15.6 standard," in *Applied Sciences in Biomedical and Communication Technologies (ISABEL), 2010 3rd International Symposium on*, nov. 2010, pp. 1 –6.

[30] Standards, "Ieee draft standard for information technology - telecommunications and information exchange between systems - local and metropolitan area networks - specific requirements - part 15.6: Wireless medium access control (mac) and physical layer (phy) specifications for wireless personal area networks (wpans)used in or around a body.," *IEEE P802.15.6/D04, June 2011*, pp. 1 –280, 27 2011.

[31] S. Ramanathan, "A unified framework and algorithms for (T/F/C)DMA channel assignment in wireless networks," in *Proc. of IEEE INFOCOM*, April 1997, pp. 900–907.

[32] R. C. Dixon, *Spread Spectrum Systems with Commercial Applications*, New York: John Wiely and Sons, third edition, 1994.

[33] IEEE Standards, "Wireless LAN Medium Access Control (MAC) and Physical Layer (PHY) Specifications," *IEEE Standard 802.11*, June 1999.

[34] C. H. Liu and H. H. Asada, "A source coding and modulation method for power saving and interference reduction in DS-CDMA sensor network systems," in *Proc. of American Control Conference*, May 2002, vol. 4, pp. 3003–3008.

[35] S. De, C. Qiao, D. A. Pados, M. Chatterjee, and S. J. Philip, "An integrated cross-layer study of wireless CDMA sensor networks," *IEEE Journal on Selected Areas in Commun.*, vol. 22, no. 7, pp. 1271–1285, Sept. 2004.

[36] T. Shu, M. Krunz, and S. Vrudhula, "Joint optimization of transmit power-time and bit energy efficiency in CDMA wireless sensor networks," *IEEE Trans. on Wireless Commun.*, vol. 5, no. 11, pp. 3109–3118, Nov. 2006.

[37] J. Y. Yu, W. C. Liao, and C. Y. Lee, "An MT-CDMA based wireless body area network for ubiquitous healthcare monitoring," in *Proc. of IEEE BioCAS*, Nov. 2006.

[38] J. G. Proakis, *Digital Communications*, New York: McGraw-Hill, forth edition, 2001.

[39] R. Poluri and A. Akansu, "Short length cdma codes for wireless sensor networks," in *Sarnoff Symposium, 2007 IEEE*, 30 2007-may 2 2007, pp. 1 –5.

[40] Keith Clayton, "Basic Concepts in Nonlinear Dynamics and Chaos," in *Society for Chaos Theory in Psychology and the Life Sciences meeting*, Marquette University, Miwaukee, Wisconsin, 1997.

[41] K. Ghanem and P.S. Hall, "Interference cancellation using cdma multi-user detectors for on-body channels," in *Personal, Indoor and Mobile Radio Communications, 2009 IEEE 20th International Symposium on*, sept. 2009, pp. 2152 –2156.

[42] K. J. Horadam, *Hadamard Matrices and Their Applications*, Princeton University Press, 2007.

[43] J. Abouei, "A set of cyclic orthogonal codes acquired from Walsh-Hadamard matrix," in *Proc. 34th International Mathematics Conference*. Shahrood, Iran, Sept. 2003.

[44] Y. Xia, P. Li, X. Shan, and Y. Ren, "Cyclically orthogonal subset of walsh functions," *The 8th International Conference on Communication Systems (ICCS)*, vol. 1, pp. 107–111, Nov. 2002.

[45] Ralf R. Mller and Johannes B. Huber, "Iterated soft-decision interference cancellation for cdma," in *in Broadband Wireless Communications, Luise and Pupolin, Eds.* 1998, pp. 110–115, Springer.

[46] Seung Hoon Park thenmozhi Arunan Euntae Won Kiran Bynam, Ranjeet Patro, "Samsungs proposal for ieee802.15.4j," July 2011.

[47] Zhongliang Deng Ning Li Pingping Xu Hao Liu Liang Li, Zhang Liang, "Dsss modulation for phy layer proposal at mban bands (ieee 802.15.4j)," May 2011.

[48] A. Zhang, L.W. Hanlen, and Xiaojing Huang, "Spreading with walsh code for pi/2-dbpsk modulated wban systems," in *Personal, Indoor and Mobile Radio Communications Workshops (PIMRC Workshops), 2010 IEEE 21st International Symposium on*, sept. 2010, pp. 84 –88.

[49] A. Mirbagheri, K.N. Plataniotis, and S. Pasupathy, "An enhanced widely linear cdma receiver with oqpsk modulation," *Communications, IEEE Transactions on*, vol. 54, no. 2, pp. 261 – 272, feb. 2006.

[50] H. T. Friis, "A note on a simple transnission formula," in *Proc. IRE*, 1946, vol. 34, pp. 245–256.

[51] H. Karl and A. Willig, *Protocols and Architectures for Wireless Sensor Networks*, John Wiley and Sons Inc., first edition, 2005.

[52] L. Barclay, *Propagation of Radiowaves*, The Institution of Electrical Engineers, London, second edition, 2003.

[53] S. Ullah and Kyung Sup Kwak, "Throughput and delay limits of ieee 802.15.6," in *Wireless Communications and Networking Conference (WCNC), 2011 IEEE*, march 2011, pp. 174 –178.

[54] S. Cui, A. J. Goldsmith, and A. Bahai, "Energy-constrained modulation optimization," *IEEE Trans. on Wireless Commun.*, vol. 4, no. 5, pp. 2349–2360, Sept. 2005.

[55] "Wireless medical telemetry service (wmts)," .

[56] Jin-Shyan Lee, Yu-Wei Su, and Chung-Chou Shen, "A comparative study of wireless protocols: Bluetooth, uwb, zigbee, and wi-fi," in *Industrial Electronics Society, 2007. IECON 2007. 33rd Annual Conference of the IEEE*, nov. 2007, pp. 46 –51.

[57] H.S. Savci, A. Sula, Z. Wang, N.S. Dogan, and E. Arvas, "Mics transceivers: regulatory standards and applications [medical implant communications service]," in *SoutheastCon, 2005. Proceedings. IEEE*, april 2005, pp. 179 – 182.

[58] Huan-Bang Li and Ryuji Kohno, "Body area network and its standardization at ieee 802.15.ban," in *Advances in Mobile and Wireless Communications*, Frigyes Istvn, Jnos Bit, and Pter Bakki, Eds., vol. 16 of *Lecture Notes in Electrical Engineering*, pp. 223–238. Springer Berlin Heidelberg, 2008.